

hZwint-1 bridges the inner and outer kinetochore: identification of the kinetochore localization domain and the hZw10-interaction domain

Larissa J. VOS*, Jakub K. FAMULSKI*¹ and Gordon K. T. CHAN*^{†‡}

*Department of Oncology, Faculty of Medicine and Dentistry, University of Alberta, 11560 University Avenue, Edmonton, Alberta, Canada, T6G 1Z2, †School of Cancer, Engineering and Imaging Sciences, University of Alberta, Edmonton, Alberta, Canada, T6G 2B7, and ‡Experimental Oncology, Cross Cancer Institute, 11560 University Avenue, Edmonton, Alberta, Canada T6G 1Z2

Accurate chromosome segregation in mitosis is required to maintain genetic stability. hZwint-1 [human Zw10 (Zeste white 10)-interacting protein 1] is a kinetochore protein known to interact with the kinetochore checkpoint protein hZw10. hZw10, along with its partners Rod (Roughdeal) and hZwilch, form a complex which recruits dynein–dynactin and Mad1–Mad2 complexes to the kinetochore and are essential components of the mitotic checkpoint. hZwint-1 localizes to the kinetochore in prophase, before hZw10 localization, and remains at the kinetochore until anaphase, after hZw10 has dissociated. This difference in localization timing may reflect a role for hZwint-1 as a structural kinetochore protein. In addition to hZw10, we have found that hZwint-1 interacts with components of the conserved Ndc80 and Mis12 complexes in yeast two-hybrid and GST (glutathione transferase) pull-down assays. Furthermore, hZwint-1 was found

to have stable FRAP (fluorescence recovery after photobleaching) dynamics similar to hHec1, hSpc24 and hMis12. As such, we proposed that hZwint-1 is a structural protein, part of the inner kinetochore scaffold and recruits hZw10 to the kinetochore. To test this, we performed mutagenesis-based domain mapping to determine which regions of hZwint-1 are necessary for kinetochore localization and which are required for interaction with hZw10. hZwint-1 localizes to the kinetochore through the N-terminal region and interacts with hZw10 through the C-terminal coiled-coil domain. The two domains are at opposite ends of the protein as expected for a protein that bridges the inner and outer kinetochore.

Key words: centromere, kinetochore, mitosis, mitotic checkpoint, Zw10, Zw10-interacting protein 1 (Zwint-1).

INTRODUCTION

Mitosis is the process by which a cell equally distributes its chromosomes into two daughter cells. Accurate chromosome segregation depends upon the bipolar attachment of kinetochores on sister chromatids to the spindle MTs (microtubules) [1]. If there is even a single unaligned chromosome, the mitotic checkpoint will delay anaphase onset until all chromosomes are attached and aligned properly [2]. The mitotic checkpoint delays anaphase by inhibiting the APC/C (anaphase-promoting complex/cyclosome), an E3 ubiquitin ligase, thus preventing the ubiquitination of proteins which need to be degraded before mitotic exit [3,4]. Loss of the mitotic checkpoint results in chromosome missegregation and may result in cell death or the formation of cancerous cells [5].

The kinetochore is a proteinaceous structure that forms on the centromere during late G₂-phase through mitosis and is responsible for MT attachment, chromosome movement and the mitotic checkpoint. The first centromere/kinetochore proteins were originally identified as the antigens recognized by antisera from patients with CREST (calcinosis, Raynaud's phenomenon, oesophageal dysmotility, sclerodactyly and telangiectasia) autoimmune disease [6]. They were designated CENP (centromere protein) A, B and C. With advances in

molecular biology techniques, additional constitutive centromere proteins have been identified and collectively are termed the CCAN (constitutive centromere-associated network) [7–9] and they create the stable scaffold upon which the kinetochore forms.

The kinetochore contains additional structural stable complexes of proteins that build the scaffold for MT attachments and checkpoint signalling, including the KMN network which is composed of the Mis12 and Ndc80 complexes and the Blinkin/KNL1 protein [10–13]. The KMN network is composed of structural inner kinetochore components which are required for recruitment of mitotic checkpoint components and stable kinetochore–MT attachments [10,14–16]. The Ndc80 complex is composed of four proteins (Hec1/Ndc80, Nuf2, Spc24 and Spc25) and is conserved from yeast to humans [17,18]. The Mis12 complex is also composed of four proteins (Mis12, Nnf1/Pmf1/Mis13, Dsn1/c20orf172/Mis14 and Nsl1/DC31) [12,19–21]. Structural kinetochore proteins localize to the kinetochore early in mitosis and are stably associated with the kinetochore to provide a scaffold for binding of outer kinetochore components such as those involved in mitotic checkpoint signalling [22,23].

Components of the mitotic checkpoint were first identified by genetic screens in yeast for mutants that did not arrest in metaphase when treated with MT-targeting drugs (MAD1–MAD3

Abbreviations used: ACA, anti-centromere antibody; AEBSF, 4-(2-aminoethyl)benzenesulfonyl fluoride; APC/C, anaphase-promoting complex/cyclosome; CCD, charge-coupled device; CENP, centromere protein; CREST, calcinosis, Raynaud's phenomenon, oesophageal dysmotility, sclerodactyly and telangiectasia; DAPI, 4',6-diamidino-2-phenylindole; DMEM, Dulbecco's modified Eagle's medium; FRAP, fluorescence recovery after photobleaching; GFP, green fluorescent protein; GST, glutathione transferase; HA, haemagglutinin; HEK, human embryonic kidney; KB, kinase buffer; KMN network, network of KNL1/Blinkin, Mis12 and Ndc80 complexes; MT, microtubule; NP40, Nonidet P40; PEI, polyethyleneimine; Rod, Roughdeal; shRNA, short hairpin RNA; siRNA, small interfering RNA; X-Gal, 5-bromo-4-chloroindol-3-yl β-D-galactopyranoside; Y2H, yeast two-hybrid; YFP, yellow fluorescent protein; Zw10, Zeste white 10; Zwint-1, Zw10-interacting protein 1.

¹ Present address: Department of Biological Sciences, University of Alberta, Edmonton, Alberta, Canada, T6G 2E9

² To whom correspondence should be addressed (email Gordon.Chan@albertahealthservices.ca).

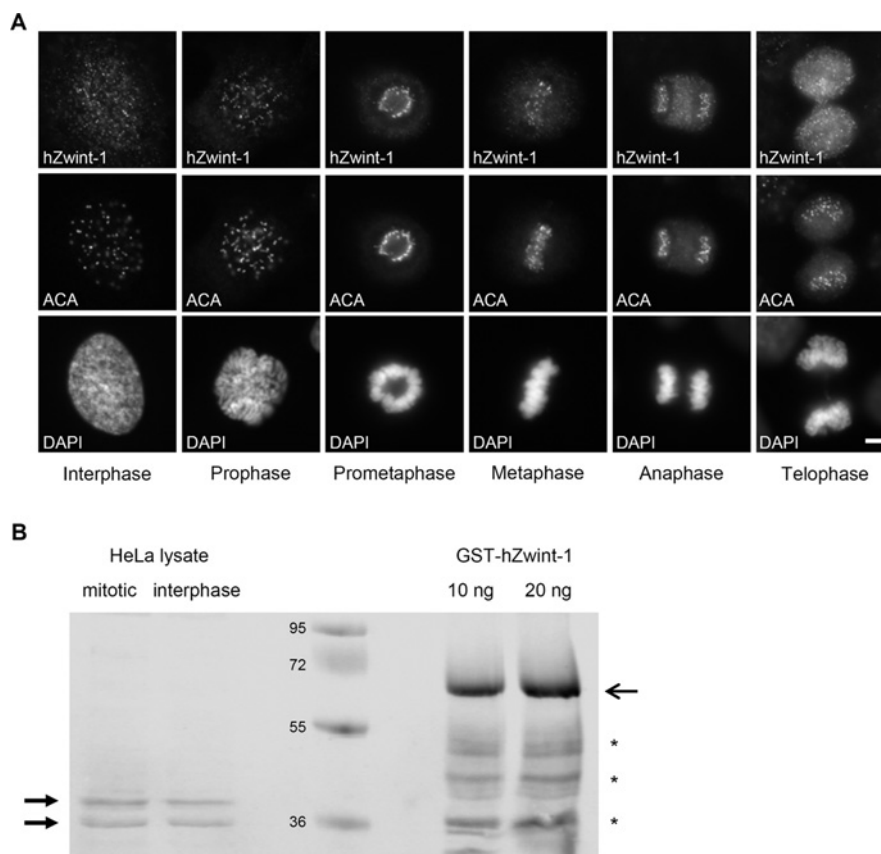


Figure 1 Anti-hZwint-1 antibody reveals that hZwint-1 localizes to the kinetochore from prophase until late anaphase

(A) HeLa cells were stained with anti-hZwint-1 antibodies, CREST antisera to stain centromeres (ACA) and DAPI to stain DNA. hZwint-1 localizes to the kinetochore from prophase until anaphase and is exterior to ACA. Each cell phase is merged in Supplementary Figure S1(C) at <http://www.BiochemJ.org/bj/435/bj435000add.htm>. Scale bar, 5 μ m. (B) Western blot analysis of anti-hZwint-1 antibody labels two bands at 38 and 40 kDa from HeLa lysate (left-hand arrows) and a 62 kDa band for recombinant GST-hZwint-1 from *E. coli* (right-hand arrow). The two bands from HeLa lysate may represent a post-translationally modified form of hZwint-1. Bands marked with asterisks are degradation products of GST-hZwint-1 that react with the anti-hZwint-1 antibody. Molecular masses are indicated in kDa.

and BUB1–BUB3). In higher eukaryotes, Mad1, Mad2, Bub1, Bub3 and BubR1 have been found to be important in the delay of anaphase in response to unattached kinetochores [24–30]. The APC/C is inhibited directly by the mitotic checkpoint complex which is composed of Cdc20, Mad2, BubR1 and Bub3 [31]. Checkpoint proteins tend to be transient components of the kinetochore with high *in vivo* FRAP (fluorescence recovery after photobleaching) rates and maximum kinetochore occupancy at unattached kinetochores during prometaphase [32].

Higher eukaryotes have additional kinetochore proteins, including hZwint-1 [human Zw10 (Zeste white 10)-interacting protein 1] [33]. hZw10 (human Zw10) along with Rod (Roughdeal) [34] and Zwilch [35] form the RZZ complex [36]. The RZZ complex is required for the recruitment of the MT motor dynein–dynactin to kinetochores and functions in the mitotic checkpoint and recruitment of the Mad1–Mad2 complex [34,37,38]. hZw10 is a dynamic component of the kinetochore at metaphase as expected for a checkpoint protein [39]. hZwint-1 localizes to the kinetochore during prophase, before hZw10, and remains until late anaphase (Figure 1A and see Supplementary Figure S1C at <http://www.BiochemJ.org/bj/435/bj435000add.htm>), after hZw10 has left, and, as such, hZwint-1 may act as a scaffold to which the human RZZ complex binds, thus recruiting it to the kinetochore. Knockdown experiments using siRNA (small interfering RNA) have shown

that when hZwint-1 is absent from the kinetochore, hZw10 is no longer able to localize to the kinetochore [40,41]. In contrast, when hZw10 is knocked down by siRNA, hZwint-1 localization to the kinetochore is not affected [41], indicating they are not interdependent. Interestingly, it has been shown that hZw10 constructs which are unable to interact with hZwint-1 are still localized to kinetochores, but have impaired checkpoint activity [39].

In the present study, we used four complementary mutagenesis techniques to map the domains of hZwint-1 that are responsible for its kinetochore localization and hZw10 interaction. In addition to hZw10, we have found that hZwint-1 also interacts with hHec1 [42], hSpc24, hSpc25 (three components of the Ndc80 complex), hMis12, hNnf1 and hDsn1 (three components of the Mis12 complex) and has been found in complex with these KMN network proteins [12,19–21,40].

EXPERIMENTAL

Cloning

The coding sequences of hZwint-1 (Gene ID: 11130), hZw10 (Gene ID: 9183), hHec1 (Gene ID: 10403), hSpc24 (Gene ID: 147841), hSpc25 (Gene ID: 57405), hMis12 (Gene ID: 79003), hNnf1 (Gene ID: 11243) and hDsn1 (Gene ID: 25936) were

amplified by PCR from the HeLa Marathon cDNA library (Clontech) using gene specific primers and cloned into a pENTR vector via restriction enzyme sites or pDONR221 by attB PCR extension and BP recombination reaction (Gateway Cloning System, Invitrogen).

Recombination of the aforementioned coding sequences and hZwint-1 mutants into Gateway expression vectors was accomplished by LR reaction (Gateway Cloning System). The destination vectors used were pcDNA-DEST47 [mammalian C-terminal GFP (green fluorescent protein) vector], pEYFP-N1-GW [mammalian C-terminal YFP (yellow fluorescent protein) vector], pEGFP-GW (mammalian N-terminal GFP vector), pCG-GW [mammalian GST (glutathione transferase) vector], pDEST15 (bacterial GST vector), pEG202-GW [Y2H (yeast two-hybrid) bait] and pJG4-5-GW (Y2H prey).

Mutagenesis

The hZwint-1 insertion mutant library was generated by transposon-mediated insertion mutagenesis (Mutation Generation System, Finnzymes). Truncation and internal deletion mutants of hZwint-1 were generated by PCR. Site-directed hZwint-1 mutants were generated by using the QuikChange[®] site-directed mutagenesis kit (Stratagene). pENTR3C hZwint-1 served as a template for all mutagenesis reactions. The mutant sequences were confirmed by sequencing using BigDye Terminators v3.1 and an ABI PRISM 310 capillary sequencer (Applied Biosciences).

Cell culture

HeLa and HEK (human embryonic kidney)-293 cells were grown as a monolayer in low-glucose DMEM (Dulbecco's modified Eagle's medium) supplemented with 100 units/ml penicillin, 100 µg/ml streptomycin, 2 mM L-glutamine and 10% (v/v) FBS (fetal bovine serum) in a humidified incubator at 37 °C with 5% CO₂. For FRAP experiments, the medium was supplemented with Hepes buffer (pH 7.4) at a final concentration of 7 mM (Invitrogen).

Western blotting

For Western blotting, HEK-293 cells were seeded at a density of 10⁵ cells/ml (2 ml) in 35-mm-diameter dishes. Cells were transiently transfected using Lipofectamine[™] 2000 (Invitrogen) according to the manufacturer's instructions or with linear PEI (polyethyleneimine) (Polysciences) as described below and harvested 24 h later and processed for Western blotting as described previously [25].

Blots were blocked with Odyssey blocking buffer (Li-Cor Biosciences) and probed with IR-800-conjugated mouse monoclonal anti-GFP antibodies (1:10000 dilution; Rockland Immunochemicals), rabbit polyclonal anti-GST (1:1000 dilution; [34]), rabbit polyclonal anti hZwint-1 (1:4000 dilution; described below) and Alexa Fluor[®] 680 anti-rabbit secondary antibody (1:10000 dilution; Invitrogen). Blots were scanned with the Odyssey IR imager system (Li-Cor Biosciences).

Fluorescence microscopy

For hZwint-1 immunofluorescence, HeLa cells were seeded on to 22 mm² coverslips at a density of 5 × 10⁴ cells/ml (2 ml) in a 35-mm-diameter dish for 24–48 h. The cells were fixed

with 3.5% (w/v) paraformaldehyde in PBS with 10 mM Pipes (pH 6.8) for 7 min. and permeabilized in KB (kinase buffer: 50 mM Tris/HCl, pH 7.4, 150 mM NaCl and 0.1% BSA) with 0.2% Triton X-100 for 5 min at room temperature (?? °C), and rinsed in KB for 5 min at room temperature. DNA was stained with 0.1 µg/ml DAPI (4',6-diamidino-2-phenylindole). Rabbit anti-hZwint-1 (1:10000 dilution) and Alexa Fluor[®] 488-conjugated anti-rabbit (1:1000 dilution; Molecular Probes) antibodies were used to detect hZwint-1. CREST patient sera were used as the primary antibody to detect the centromere [ACA (anti-centromere antibody)] (1:4000 dilution, a gift from Dr Marvin Fritzler, University of Calgary, Calgary, AB, Canada) and Alexa Fluor[®] 647 anti-human secondary antibody (1:1000 dilution; Molecular Probes). Coverslips were mounted with 1 mg/ml Mowiol 4-88 (Calbiochem) in phosphate buffer (pH 7.4).

For fluorescence microscopy of GFP-tagged constructs, HeLa cells were seeded on to 22 mm² coverslips at a density of 5 × 10⁴ cells/ml (2 ml) in 35-mm-diameter dishes and grown for 24 h before transfection. Cells were transiently transfected for 24 h using Lipofectamine[™] 2000 according to the manufacturer's instructions or with PEI as described below and fixed and permeabilized as described above. DNA was stained with DAPI (0.1 µg/ml), and coverslips were mounted with Mowiol 4-88 (Calbiochem).

Cells were visualized with a 100× Plan-Apochromatic objective on a Zeiss AxioPlan 2 microscope. Images were captured with a Photometrics CoolSNAP HQ CCD (charge-coupled device) camera (Roper Scientific) controlled by Metamorph 6.0 software (Universal Imaging Corporation). Image processing was performed using Adobe Photoshop 7.0.

PEI transfection

For each transfection, 2 µg of plasmid DNA was diluted in 150 µl of Opti-MEM[®] and mixed. In a separate tube, 10 µl of PEI (1 mg/ml) was combined with 100 µl of Opti-MEM[®] per sample, mixed and incubated at room temperature for 5 min. The diluted PEI and diluted plasmid solutions were combined, vortex-mixed and incubated for 15 min at room temperature to allow complexes to form. The plasmid-PEI complexes were added to each dish containing cells and fresh low-glucose DMEM and were gently rocked to mix.

Yeast two-hybrid assays

Y2H assays were performed as described previously [25]. Briefly, the yeast was co-transformed with full-length hZw10 fused to the LexA DNA-binding domain, and hZwint-1 wild-type or mutants fused to the LexA activation domain and the lacZ reporter plasmid. Transformants were selected using drop-out medium. Expression of baits and preys were confirmed by Western blotting. LexA-fusion proteins were detected with a rabbit polyclonal anti-LexA antibody (1:1000 dilution; Invitrogen) and Alexa Fluor[®] 680-conjugated anti-rabbit secondary antibody (1:10000 dilution; Molecular Probes). The HA (haemagglutinin)-fusion proteins were detected with a mouse monoclonal anti-HA antibody (1:500 dilution; 12CA5; Covance Research Products) and IR-Dye800 anti-mouse (1:10000 dilution; Rockland Immunochemicals). Colonies that had fusion protein expression were streaked on to –His/–Ura/–Trp galactose/raffinose X-Gal (5-bromo-4-chloroindol-3-yl β-D-galactopyranoside) dropout agar plates. The plates were analysed 24 and 48 h later for blue/white scoring of interaction. The wild-type interaction screen was performed by

cloning full-length coding sequences into both the prey and bait plasmids and co-transforming pairs as described above.

Yeast strains EGY473 and SKY191 and the plasmids pJG4-5-GW, pEG202-GW and pSH18-34 were provided by Dr Erica Golemis (Fox Chase Cancer Center, Philadelphia, PA, U.S.A.).

GST pull-down

HEK-293 cells were seeded at a density of 10^5 cells/ml (5 ml) in 60-mm-diameter dishes. After 24 h, cells were co-transfected with 2 μ g each of GST-tagged and GFP-tagged constructs using 20 μ l of linear PEI and were harvested 24–36 h later in 400 μ l of NP40 (Nonidet P40) lysis buffer. A 5% portion of each lysate was analysed by Western blotting. The protein amount was determined based upon band intensity, and the remaining lysate was normalized to have an equal concentration of the GFP-tagged protein.

The GST pull-down was performed with glutathione–Sephadex 4B (GE Healthcare) beads blocked with 1% (w/v) BSA and stored as a 50% slurry in 1% NP40 lysis buffer with 10 μ g/ml AEBSEF [4-(2-aminoethyl)benzenesulfonyl fluoride]. A 5% portion of the normalized lysate was reserved as an initial sample. The remaining normalized lysate was incubated with 30 μ l of glutathione bead slurry for 1–4 h at 4 °C on a rotator. The beads were pelleted, and 5% of the supernatant was transferred to a new tube. The beads were washed five times with 1 ml of 1% NP40 lysis buffer with AEBSEF. The beads were pelleted and then resuspended in 30 μ l of SDS sample buffer. The samples were stored at –80 °C until analysed by Western blotting. GST alone was used as a control in each experiment to ensure that the beads or GST alone do not pull-down hZwint-1–GFP.

GST–hZwint-1 protein and anti-hZwint-1 antibody production

Recombinant GST–hZwint-1 fusion protein expression was induced in the *Escherichia coli* strain BL21 DE3 codon+. The soluble GST-fusion protein was purified with a glutathione–Sephadex 4B column and used as an antigen for immunization of rats and a rabbit. Antibodies were purified by pre-absorbing the sera on to an Affigel 15 column (Bio-Rad Laboratories) that was covalently coupled to bacterial lysate containing GST to deplete antibodies against GST and bacterial proteins. Anti-hZwint-1 antibodies were purified by passing the pre-absorbed sera through an Affigel 15 column that was covalently coupled to GST–hZwint-1 fusion protein. Antibodies were eluted and concentrated as described previously [43].

FRAP

For FRAP, HeLa cells were seeded on to glass-bottomed 35 mm dishes (World Precision Instruments) at a density of 5×10^4 cells/ml (2 ml) for 24 h before transfection. Cells were transiently transfected with pEGFP-GW or pEYFP-N1-GW fluorescently tagged constructs using Lipofectamine™ 2000 according to the manufacturer's instructions. FRAP was performed as described previously [39].

Quantification of hZwint-1 fluorescence intensity

Coverslips were generated as described above. Cells were visualized with a 100 \times Plan-Apochromatic objective on a Zeiss AxioPlan 2 microscope. Images were captured with a Photometrics CoolSNAP HQ CCD camera controlled by

Metamorph 6.0 software. Quantification of hZwint-1 fluorescence intensity at different mitotic stages was performed using Metamorph 6.0 software. Briefly, fluorescence intensities at kinetochores were measured within a nine-pixel diameter circle followed by background subtraction from a larger 15-pixel diameter circle of the same region. A total of 30 in-plane kinetochores were examined for each mitotic phase. Kinetochores fluorescence values were averaged for each mitotic phase and the S.D. values were calculated and graphed using Microsoft Excel.

RESULTS

hZwint-1 is a 38 kDa protein which localizes to the kinetochore from prophase through anaphase

Although hZwint-1 was identified as a kinetochore component in 2000 [33], there were no commercial antibodies available at the onset of the present study. As such, we produced bacterially expressed GST–hZwint-1 and an antibody against hZwint-1 was generated and affinity-purified. It was tested for its ability to detect endogenous and recombinant hZwint-1 on a Western blot (Figure 1B). The antibody detected a set of bands at 38 and 40 kDa from interphase and mitotic HeLa extracts. This is larger than the predicted molecular mass of hZwint-1 (31.2 kDa), but lower than described previously (43 kDa) [33]. We are confident that our antibody is detecting two forms of endogenous hZwint-1, as the bands are consistent with the size of bacterially expressed hZwint-1 [12] and both bands are reduced following siRNA treatment (results not shown). The antibody recognized a dominant band at 64 kDa in the lanes loaded with the bacterially expressed GST–hZwint-1.

To examine the specificity of our antibody for immunofluorescence, we examined the distribution of hZwint-1 in mitotic HeLa cells by immunofluorescence microscopy and found that it was first detected at kinetochores in prophase, before nuclear envelope breakdown, and persisted through anaphase A (Figure 1A), which is consistent with results published previously [33]. The localization pattern of hZwint-1 was confirmed by transfection of HeLa cells with a GFP-fusion construct of hZwint-1. Analysis of GFP–hZwint-1 revealed that fusion of GFP to the N-terminus of hZwint-1 prevented the wild-type protein from localizing to the kinetochore. When GFP was fused to the C-terminus of hZwint-1, the fusion construct was able to localize to the kinetochore with the same timing as seen for endogenous hZwint-1 (see Supplementary Figure S1A).

The kinetochore localization domain of hZwint-1 is within the N-terminus

Several studies have examined the regions within hZwint-1 that are involved in hZwint-1 interaction and kinetochore localization [33,39,41] but none have examined the domains within hZwint-1 which determine kinetochore localization. In order to determine the kinetochore localization domain of hZwint-1, we generated both N- and C-terminal truncations fused to GFP and transiently transfected them into HeLa cells. Analysis of these truncation mutants revealed that regions in both the N- and C-termini are required for kinetochore localization. Although deleting the first 40 amino acids of hZwint-1 did not affect kinetochore localization (mutants C1–C4), removal of 80 or more amino acids from the N-terminus resulted in the loss of kinetochore localization (Figure 2A and Table 1). Truncations from the C-terminus of the protein showed that mutant N3 (amino acids 1–228) was negative for kinetochore localization, but removal

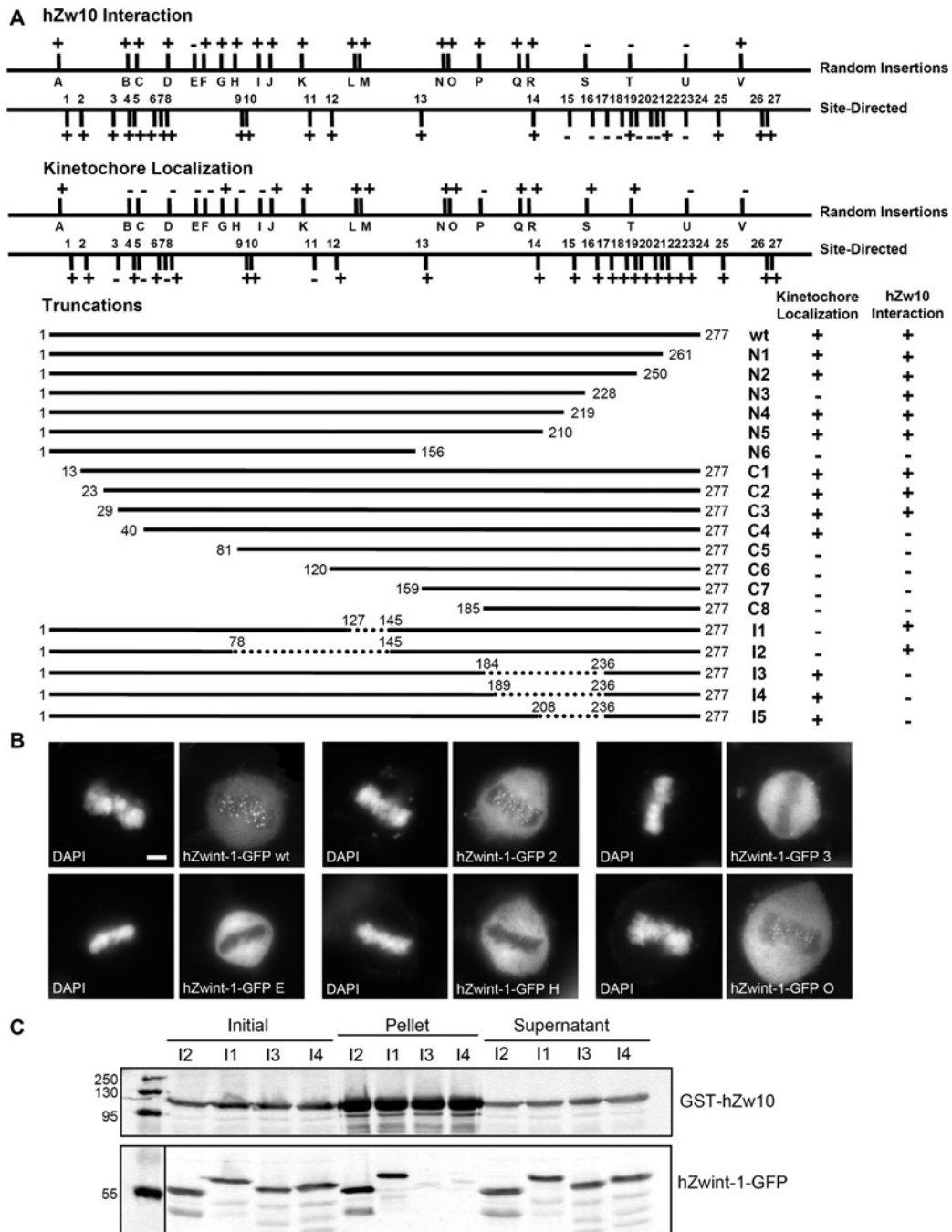


Figure 2 hZwint-1 localizes to the kinetochore through a region in its N-terminus and interacts with hZw10 through its C-terminus

(A) Schematic diagram of the hZwint-1 mutant library with ability to localize to the kinetochore (Knt. Loc.) (+) or not localized (-) and ability (+) or inability (-) to interact with hZw10 (Zw10 Int.) indicated. The kinetochore localization domain of hZwint-1 is in the N-terminal region of the protein with amino acids 40–109 being necessary, but not sufficient, for kinetochore localization of hZwint-1. The first coiled coil of hZwint-1 is also important in kinetochore localization. For hZw10 interaction, mutants are considered negative if they are unable to or have reduced ability to interact with hZw10 in Y2H assays or if they are not pulled down by GST-hZw10 or if negative in both assays. The C-terminal amino acids 195–236 of hZwint-1 are necessary, but not sufficient, for interaction with hZw10. For detailed mutation information, see Tables 1–4. (B) Examples of mutants from the N-terminal region showing both positive and negative kinetochore localization. HeLa cells were transfected with hZwint-1-GFP fusion constructs, fixed, stained with DAPI to visualize the DNA and examined by fluorescence microscopy for ability to localize to the kinetochore. For fluorescence pictures of all mutants, see Supplementary Figures S3–S5 at <http://www.BiochemJ.org/bj/435/bj4350000add.htm>. Expression of mutants was confirmed by Western blot analysis (see Supplementary Figure S2 at <http://www.BiochemJ.org/bj/435/bj4350000add.htm>). Scale bar, 5 μ m. (C) Representative Western immunoblot from GST pull-down experiment of internal deletion mutants with an example of mutants that are able to be pulled down and mutants that are no longer able to be pulled down by GST-hZw10. Full pull-down data can be found in Tables 1–4. GST-hZw10 is able to pull-down hZwint-1-GFP internal deletion mutants I1 and I2, but not I3 and I4, confirming the role of the second coiled-coil domain in hZwint-1 interaction with hZw10. Initial samples are 5% of lysate before addition of glutathione-Sepharose beads, pellet is total bound proteins and supernatant is 5% of lysate after beads were pelleted. GFP-fusion proteins were detected with IR800-conjugated anti-GFP antibody and GST-fusion proteins were detected with rabbit anti-GST primary antibody and Alexa Fluor[®] 680-conjugated anti-rabbit secondary antibody. The two blot images are from different channels of the same blot. The molecular-mass protein ladder (masses indicated in kDa) only shows up in the 700 channel and has been placed beside the GFP 800 channel blot for reference.

Table 1 hZwint-1 truncation mutants

Interaction between hZw10 and hZwint-1 truncation constructs was analysed with the LexA Y2H system using X-Gal and by GST pull-down. Kinetochores localization was examined through fluorescence microscopy analysis of GFP-fusion constructs. Yeast colonies were scored for appearance of blue colour 2 and 3 days after streaking out. Each combination of interactions was redone in three separate experiments and confirmed for expression of fusion constructs by Western blotting with anti-HA and anti-LexA antibodies (results not shown). The possibility of false positives was checked by transformation of bait construct with empty prey vector and prey construct with empty bait vector. Transfection of the empty GST vector with GFP constructs was used for control of false pull-downs.

Construct	Amino acids encoded	Y2H with hZw10	GST pull-down with hZw10	Kinetochores localization
N1	1–261	Positive	Positive	Positive
N2	1–250	Positive	Positive	Positive
N3	1–228	Positive	Positive	Negative
N4	1–219	Positive	Positive	Positive
N5	1–210	Positive	Positive	Positive
N6	1–156	Negative	Negative	Negative
C1	13–277	Positive	Positive	Positive
C2	23–277	Positive	Positive	Positive
C3	29–277	Positive	Positive	Positive
C4	40–277	Negative	Negative	Positive
C5	81–277	Positive	Negative	Negative
C6	120–277	Positive	Negative	Negative
C7	159–277	Negative	Negative	Negative
C8	185–277	Negative	Negative	Negative

of additional amino acids [N4 (amino acids 1–219) and N5 (amino acids 1–210)] restored localization to the kinetochore. The inability of mutant N3 to localize to the kinetochore is not caused by lack of expression as all mutants expressed at the expected size on Western blot (see Supplementary Figure S2 at <http://www.BiochemJ.org/bj/435/bj4350000add.htm>) and showed GFP expression when examined by fluorescence microscopy (Figure 2B and see Supplementary Figures S3–S5 at <http://www.BiochemJ.org/bj/435/bj4350000add.htm>).

Truncation analysis may generate problems with protein secondary structure and give false negatives, so we performed localized disruptions by transposon-mediated random insertion mutagenesis, resulting in 15 bp in-frame insertions spread along the coding sequence. Examining the ability of these 22 random insertion GFP-fusion mutants to localize to the kinetochore revealed a cluster of mutants in the N-terminus (B–F, H and I) as well as two mutants (U and V) in the far C-terminus and one in the middle (P) that were not able to localize to the kinetochore (Figure 2A and Table 2). To validate further the random insertion results, we generated small site-directed mutants concentrated in the N- and C-termini of hZwint-1 (Figure 2A and Table 3). To determine whether the coiled-coil domains of hZwint-1 were involved in kinetochore localization, we also generated internal deletions (Figure 2A and Table 4) which removed part or all of the first or second coiled coil. Fluorescence microscopy of these mutants further supports the role of the N-terminus in kinetochore localization. Examination of the random insertion and site-directed mutant library demonstrates that amino acids 40–109 are necessary for kinetochore localization. Inclusion of the internal deletions and truncations expands the domain to amino acids 40–145 being necessary, but not sufficient, for kinetochore localization.

hZwint-1 interacts with hZw10 through the C-terminal coiled-coil region

Interaction between hZw10 and hZwint-1 is required for the stable recruitment and checkpoint activity of hZw10 [39] and, although

Table 2 hZwint-1 random insertion mutants

The sequence and exact site of insertion were verified by sequencing. Interaction between hZw10 and hZwint-1 site-directed constructs was analysed with the LexA Y2H system using X-Gal and by GST pull-down assay. Kinetochores localization was examined through fluorescence microscopy analysis of GFP-fusion constructs. Positive indicates medium blue colour after 2 or 3 days for Y2H and positive indicates equivalent interaction to the ability of the wild-type construct for GST pull-down analysis. Weak indicates light blue colour after 2 or 3 days for Y2H and ~50% interaction compared with wild-type for GST pulldown analysis. Controls are as in Table 1.

Construct	Insertion	Y2H with hZw10	GST pull-down with hZw10	Kinetochores localization
A	A ¹² AAPS	Positive	Positive	Positive
B	R ⁴³ PQFV	Positive	Positive	Negative
C	L ⁴⁶ RPHS	Positive	Positive	Negative
D	R ⁶⁷ PHQL	Positive	Positive	Negative
E	V ⁶⁷ RPHL	Negative	Positive	Negative
F	Q ⁶⁸ VRPH	Positive	Positive	Negative
G	A ⁷⁵ AAKG	Positive	Positive	Positive
H	A ⁸⁰ AALG	Positive	Positive	Negative
I	A ⁸⁸ CGRK	Positive	Positive	Negative
J	V ⁹³ RPHK	Positive	Positive	Positive
K	V ¹⁰⁴ RPHR	Positive	Positive	Positive
L	D ¹²¹ AAAM	Positive	Positive	Positive
M	A ¹²² AAAME	Positive	Positive	Positive
N	Q ¹⁵² MRPH	Positive	Positive	Positive
O	M ¹⁵³ RPHQ	Positive	Positive	Positive
P	L ¹⁶⁵ RPQQ	Positive	Positive	Negative
Q	T ¹⁷⁸ GAAA	Positive	Weak	Positive
R	A ¹⁸⁰ AAPG	Positive	Positive	Positive
S	V ²⁰¹ RPQQ	Negative	Negative	Positive
T	C ²¹⁶ GRIL	Negative	Negative	Positive
U	C ²³⁶ GRIP	Negative	Positive	Negative
V	A ²⁵⁶ AAMG	Positive	Positive	Negative

several studies have mapped the domains of hZw10 required for hZwint-1 interaction, the regions of hZwint-1 involved in binding hZw10 have not been fully examined. Lin et al. [42] performed *in vitro* binding assays between full-length GST-hZwint-1 or the individual coiled coils with hHec1 or hZw10 and found that the first coiled coil (amino acids 80–155) was sufficient for both hZw10 and hHec1 interaction. To elucidate further the domain of hZwint-1 responsible for hZw10 interaction, we employed the aforementioned mutant library in two complementary assays. We performed Y2H assays to analyse hZw10 interaction with hZwint-1 wild-type and mutants, as well as GST pull-down of GFP-fusion constructs from HEK-293 cell lysates.

Examination of the truncation mutants by Y2H revealed that all C-terminal truncation mutants were able to interact with hZw10 except for N6 (amino acids 1–156) (Figure 2A and Table 1). Analysis of the N-terminal truncations revealed three mutants which lost interaction, C4 (amino acids 40–277), C7 (amino acids 159–277) and C8 (amino acids 185–277); however, mutants C5 (amino acids 81–277) and C6 (amino acids 120–277) were still able to interact with hZw10. This suggests that C4 may be negative because of altered secondary structure of the protein rather than loss of the interaction domain. On the basis of the truncations, amino acids 30–210 appear to contain the hZw10-interaction domain. To narrow down the domain, the random insertion mutant library was screened and revealed four mutants that were unable to interact with hZw10. Of these mutants, three were in the C-terminus [mutant S (V²⁰¹RPQQ), mutant T (C²¹⁶GRIL) and mutant U (C²³⁶GRIP)] and the fourth was in the N-terminus of the protein [mutant E (V⁶⁷RPHL)] (Figure 2A and Table 2). More refined examination of the C-terminal region with site-directed mutants (Figure 2A and Table 3) narrowed the N-terminal boundary to

Table 3 hZwint-1 site-directed mutants

All of the point mutations were verified by sequencing. Interaction between hZw10 and hZwint-1 site-directed constructs was analysed with the LexA Y2H system using X-Gal and by GST pull-down assay. Kinetochore localization was examined through fluorescence microscopy analysis of GFP-fusion constructs. Positive indicates medium blue colour after 2 or 3 days for Y2H and ~50% interaction compared with wild-type for GST pull-down analysis; n.d., not determined. Controls are as in Table 1.

Construct	Mutation	Y2H with hZw10	GST pull-down with hZw10	Kinetochore localization
1	ΔE ²⁴ PV ²⁶	Positive	Positive	Positive
2	Q28A/E29A	Positive	Positive	Positive
3	Δ ⁴⁰ VEF ⁴²	Positive	Positive	Negative
4	S46A	Positive	Positive	Positive
5	ΔS ⁴⁶ QK ⁴⁹	Positive	Positive	Negative
6	C54S	Positive	Positive	Positive
7	ΔQ ⁵⁶ LQ ⁵⁸	Positive	Positive	Negative
8	Q58E	Positive	Positive	Positive
9	S85A	Positive	Positive	Positive
10	ΔS ⁸⁵ RQ ⁸⁷	Positive	Positive	Positive
11	ΔV ¹⁰⁷ EA ¹⁰⁹	Positive	Positive	Negative
12	I112C	Positive	Positive	Positive
13	A145P	Positive	Positive	Positive
14	ΔT ¹⁸¹ QQELDG ¹⁸⁷	n.d.	Positive	Positive
15	ΔK ¹⁹⁶ QQ ¹⁹⁸	Positive	Negative	Positive
16	ΔD ²⁰⁴ K ²⁰⁵	Negative	Negative	Positive
17	ΔQ ²¹⁰ TF ²¹²	Positive	Weak	Positive
18	ΔQ ²¹⁴ LL ²¹⁶	Weak	Negative	Positive
19	Y217C	Positive	Positive	Positive
20	ΔT ²¹⁸ LQ ²²⁰	Negative	Negative	Positive
21	L223S/F224S	Negative	Positive	Positive
22	ΔP ²²⁶ E ²²⁷	Weak	Positive	Positive
23	ΔP ²²⁶ EAEAEENL ²³⁵	n.d.	Positive	Positive
24	P235A/D236A	Negative	Positive	Positive
25	ΔQ ²⁴⁷ EQ ²⁴⁹	Positive	Positive	Positive
26	S262A	Positive	Positive	Positive
27	ΔS ²⁶² FK ²⁶⁴	Positive	Positive	Positive

Table 4 hZwint-1 internal deletion mutants

Interaction between hZw10 and hZwint-1 internal deletion constructs was analysed with the GST pull-down assay, with controls as in Table 1. Kinetochore localization was examined through fluorescence microscopy analysis of GFP-fusion constructs.

Construct	Deletion	GST pull-down with hZw10	Kinetochore localization
I1	Δ127–145	Positive	Negative
I2	Δ78–145	Positive	Negative
I3	Δ184–236	Negative	Positive
I4	Δ189–236	Negative	Positive
I5	Δ208–236	Negative	Positive

amino acid 196, but expanded the hZw10-interaction domain to amino acids 196–236.

These results were confirmed with mammalian GST pull-down assays. Location of the GFP tag on hZwint-1 did not affect its ability to be pulled down by GST–hZw10 (see Supplementary Figure S1B). Truncation analysis was similar to the Y2H results except that C5 (amino acids 81–277) and C6 (amino acids 120–277) were negative for pull-down (Table 1). GST–hZw10 pull-down of the random insertion mutants was also very similar to the Y2H results except that E (V⁶⁷RPHL) and U (C²³⁶GRIP) were positive for pull-down, but negative in the Y2H assay (Table 2). GST pull-down examination of the site-directed mutants indicated that fewer of the mutants were negative compared with the Y2H assay; however, those that were negative were within the same region as the negative Y2H mutants (Table 3).

Internal deletion mutants removing the coiled-coil domains were examined and support the role of the C-terminus of hZwint-1 in hZw10 interaction (Figure 2C and Table 4). Amino acids 196–236 are necessary, but not sufficient, for hZw10 interaction.

hZwint-1 interacts with several inner kinetochore proteins in the KMN network

Several groups have examined the interactions within the KMN network. Direct interaction between hZwint-1 and both Blinkin [12] and Hec1 [42] have been demonstrated. To determine which protein in the KMN network is responsible for the kinetochore localization of hZwint-1, we performed Y2H analysis between hZwint-1 and several of the KMN network proteins. We found that, in addition to hZw10, hZwint-1 interacts with hHec1, hSpc24, hSpc25 (three members of the highly conserved Ndc80 complex), hMis12, hNnf1 and hDsn1 (three components of the conserved Mis12 complex) by Y2H (Table 5 and see Supplementary Figure S6 at <http://www.BiochemJ.org/bj/435/bj4350000add.htm>) as well as mapping interactions between these proteins. The interaction between hZwint-1 and the Mis12 and Ndc80 complex members was confirmed by GST pull-down assay (Figure 3 and Table 6).

hZwint-1 is a stable component of the kinetochore

The majority of the proteins that hZwint-1 interacts with are structural proteins of the inner kinetochore and have been found to be stable components with slow or no recovery after photobleaching. To examine whether hZwint-1 behaves similarly to the KMN network (stable) [23,44] and is a structural component or similarly to hZw10 (dynamic) [39] and is a checkpoint component, we performed FRAP analysis.

HeLa cells were transfected with a plasmid expressing hZwint-1–YFP and fluorescence recovery at the kinetochore was followed after laser photobleaching. We found that hZwint-1–YFP does not recover at prometaphase or metaphase kinetochores after photobleaching (Figure 4A), even when examined at extended time points (e.g. 10 min). A typical recovery curve for hZwint-1–YFP is shown in Figure 4(B). The low level of recovery seen is probably due to diffusion of soluble hZwint-1–YFP into the bleached region and not true recovery at the kinetochore. Thus we conclude that hZwint-1 is a stable kinetochore protein. GFP–hMis12, GFP–hHec1 and GFP–hSpc24 were also found to be stable kinetochore components by FRAP analysis (see Supplementary Figure S7 at <http://www.BiochemJ.org/bj/435/bj4350000add.htm>).

Another measure of protein dynamics is the relative fluorescence intensity changes at a particular location during the cell cycle [32]. Individual HeLa kinetochore intensity measurements of hZwint-1 fluorescence revealed that hZwint-1 signal becomes enriched at kinetochores through prophase and prometaphase, the intensity peaks at metaphase and remains high through anaphase A and then decreases at anaphase B and is absent at late telophase (Figure 4C). These results confirm that hZwint-1 is a stable structural component of the kinetochore.

DISCUSSION

We generated a library of hZwint-1 mutants which were used to map the kinetochore localization domain of hZwint-1 to the N-terminus of the protein. By employing the mutant library in Y2H and GST pull-down assays, we mapped the hZw10-interaction

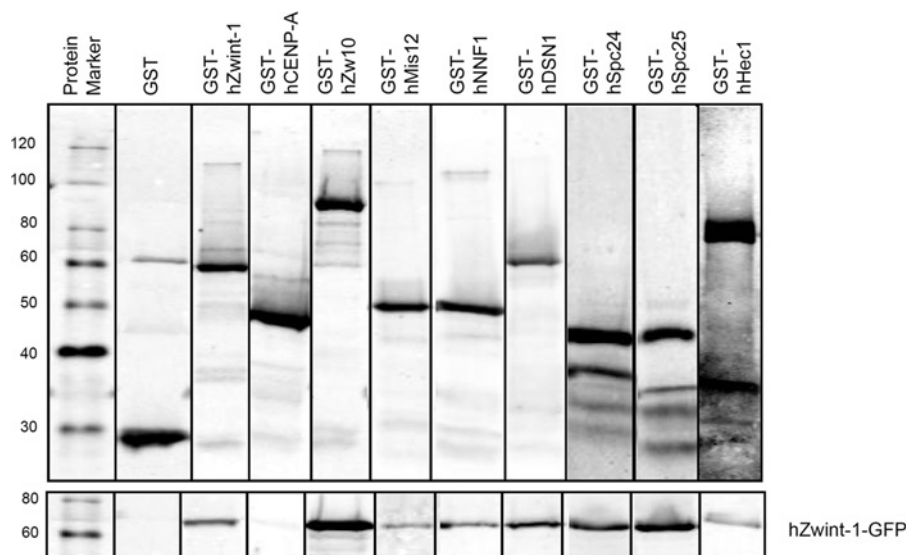


Figure 3 hZwint-1 interacts with several kinetochore components

Representative panels from Western blots examining interactions by pull-down of hZwint-1-GFP with GST-fusion constructs. hZwint-1 is able to be pulled down by hZw10, hHec1, hSpc24, hSpc25, hMis12, hNnf1, hDsn1 and itself, but not by CENP-A or GST alone. Summary of interactions by GST pull-down are in Table 6. Molecular masses are indicated in kDa.

Table 5 Wild-type protein–protein interactions assessed by Y2H

Interaction between kinetochore constructs was analysed with the LexA Y2H system using X-Gal. The possibility of false positives was checked by transformation of bait construct with empty prey vector and prey construct with empty bait vector. The strength of interaction was examined as follows: +, weak interaction (colony is light blue after 3 days); ++, medium interaction (colony is medium blue after 3 days); +++, strong interaction (colony is blue after 1 day and deep blue after 3 days); –, no interaction (colony is still white after 3 days); n.d., not determined.

Prey	Bait							
	hZwint-1	hHec1	hSpc24	hSpc25	hMis12	hNnf1	hDsn1	hZw10
hZwint-1	+++	+++	+++	–	+	++	+	++
hHec1	–	–	++	–	–	n.d.	n.d.	n.d.
hSpc24	++	+	+++	n.d.	–	n.d.	n.d.	n.d.
hSpc25	++	n.d.	n.d.	n.d.	n.d.	n.d.	n.d.	n.d.
hMis12	+++	++	+++	++	++	+++	+	n.d.
hNnf1	+++	n.d.	n.d.	n.d.	++	+++	–	n.d.
hDsn1	+++	n.d.	n.d.	n.d.	++	++	++	n.d.
hZw10	–	n.d.	n.d.	n.d.	n.d.	n.d.	n.d.	n.d.
hCENP-A	–	n.d.	n.d.	n.d.	n.d.	n.d.	n.d.	n.d.

Table 6 Wild-type protein–protein interactions assessed by GST pull-down

Interaction between kinetochore constructs was analysed with the GST pull-down assay. The ability of GST-fusion constructs to pull down hZwint-1-GFP fusion was assayed by Western blot analysis.

GST-fusion protein	Interaction with hZwint-1-GFP
GST-hZwint-1	Positive
GST-hHec1	Positive
GST-hSpc24	Positive
GST-hSpc25	Positive
GST-hMis12	Weak
GST-hNnf1	Positive
GST-hDsn1	Positive
GST-hZw10	Positive
GST-hZwilch	Positive
GST-hCENP-A	Negative

domain to the C-terminus of hZwint-1. These two domains are at opposite ends of the protein as expected because hZw10 is an outer kinetochore protein, whereas other hZwint-1 interactors (e.g.

hMis12) are inner kinetochore proteins. No obvious dominant-negative phenotypes were observed when either of these domains was disrupted. Our results show that hZwint-1-GFP is a stable component of the kinetochore with similar FRAP dynamics as three components of the KMN network (hMis12, hHec1 and hSpc24). As such, hZwint-1 is a scaffold protein which bridges the inner and outer kinetochore components.

hZwint-1 kinetochore localization domain is in the N-terminus

On the basis of the random insertion and site-directed mutants, the kinetochore localization domain of hZwint-1 was mapped to amino acids 40–109 in the N-terminus of the protein. There are mutants outside this region that are no longer able to localize to the kinetochore, but the majority of kinetochore localization-negative mutants were clustered in this region. Analysis of the truncation mutants suggested a role for both the N- and C-termini of hZwint-1 in kinetochore localization. One reason for this may be that hZwint-1 is a small protein with two predicted coiled-coil domains (see Supplementary Figure S8B

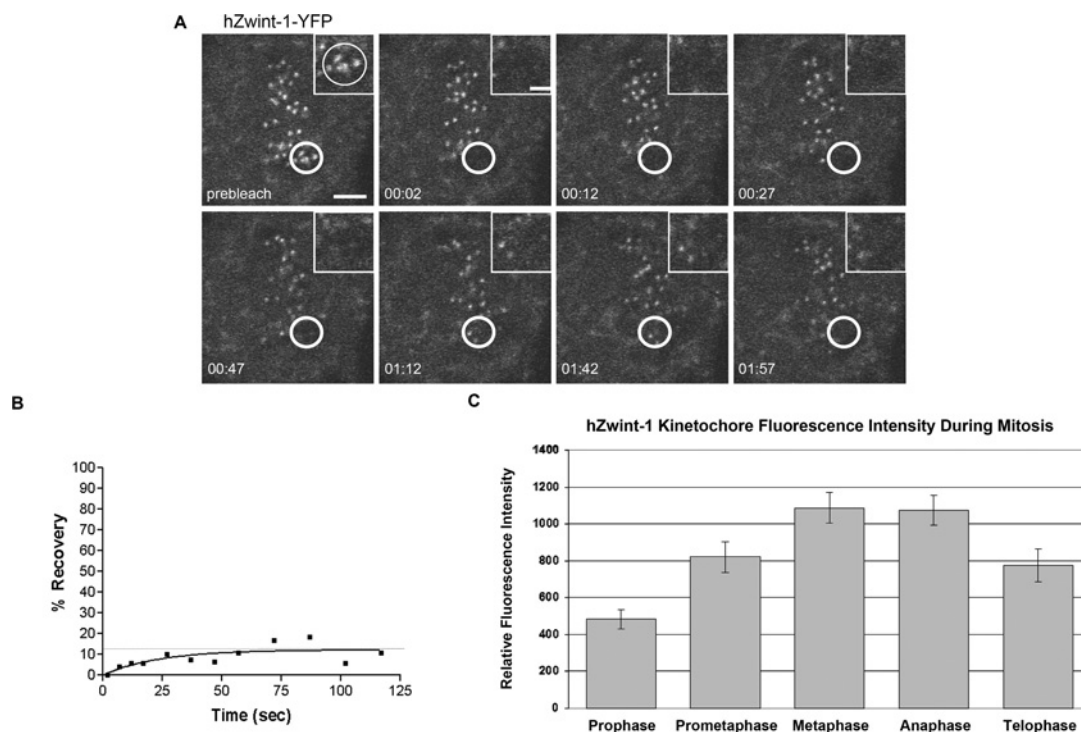


Figure 4 hZwint-1 is a stable kinetochore component

(A) Stills from a live-cell photobleaching movie. The area bleached is indicated by a circle on each image. The time of image acquisition is indicated on each panel (min:s) with laser photobleaching occurring at time 00:00. Large scale bar, 10 μm ; inset scale bar, 5 μm . (B) Fluorescence recovery following laser photobleaching. Maximum recovery was 12% of initial signal within the bleached area. The lack of fluorescence recovery for hZwint-1 is in contrast with our previous findings for GFP-hZw10 which showed rapid recovery with a $t_{1/2}$ of 13.8 ± 5.2 s [39]. (C) hZwint-1 fluorescence intensity at individual HeLa kinetochores over the mitotic phases. Results are means \pm S.D. ($n = 30$). hZwint-1 localizes to the kinetochore at prophase and remains until late anaphase/early telophase, with peak fluorescence intensity in metaphase and anaphase.

at <http://www.BiochemJ.org/bj/435/bj4350000add.htm>) and, as such, truncating the protein may disrupt its structure, resulting in a loss of localization. Random insertion mutagenesis is less disruptive to overall secondary structure than truncations, but one thing that needs to be considered is the possibility of introducing a proline residue which could disrupt the secondary structure of the protein. Whereas introduction of a proline could explain outlying mutants P (L¹⁶⁵RPQQ) and U (C²³⁶GRIP), mutant V (A²⁵⁶AAMG) does not introduce a proline and yet is negative for kinetochore localization. The location of this mutant is in the far C-terminus of the protein which is not conserved among mammals and is absent from the mouse and rat Zwint-1 homologues (see Supplementary Figure S8A). As such, it is unlikely to be involved in a conserved function such as kinetochore localization. The region with high density of kinetochore localization-negative mutants is within a well-conserved region of Zwint-1 and is located N-terminal to and containing a small portion of the first coiled-coil of hZwint-1 (see Supplementary Figure S8B). Deletion of the entire (I2) or a small piece (II) of the first coiled coil of hZwint-1 prevented kinetochore localization, but this may be due to disruption of the secondary structure, as random insertion mutants J (V⁹³RPHK) and K (V¹⁰⁴RPHR) retain kinetochore localization, although they introduce a proline residue that would disrupt the coiled coil.

The hZw10-interaction domain of hZwint-1 is in the C-terminus

Analysis of the mutant library for interaction with hZw10 through Y2H and mammalian GST pull-down assays revealed a region between amino acids 196 and 236 involved in binding hZw10.

The truncation mutants suggested a role for both the N- and C-termini of hZwint-1 as with the kinetochore localization domain mapping. The random insertion mutants had one mutant that was outside the cluster of mutants in the C-terminus, mutant E (V⁶⁷RPHL). Although this result may point to a role of the N-terminus in the hZw10 interaction, we believe that it is more likely the result of altered secondary structure of mutant E. This insertion mutant introduces a proline residue which would disrupt the first coiled coil of hZwint-1. In addition, this mutant is negative for kinetochore localization and for interaction in all Y2H screens performed [e.g. Hec1 (results not shown)]. The hZw10-interaction domain mapped in the present study is located within the C-terminal region of the second coiled-coil domain and within a highly conserved region of Zwint-1 (see Supplementary Figures S8A and S8B).

Our domain mapping of the hZw10-interaction domain is not in agreement with that published previously. It was found previously that hZwint-1 interacts with both Hec1 and Zw10 through the first coiled coil of hZwint-1 by *in vitro* binding assays using bacterially expressed recombinant proteins [42]. Neither the kinetochore localization nor the hZw10-interaction domains identified in the present study are solely within the first coiled coil of hZwint-1, although it may contribute to kinetochore localization. In an attempt to reconcile these results, we made additional hZwint-1 mutants consisting of the first coiled coil, the second coiled coil and both coiled-coil regions. These mutants were employed in the Y2H assay, and only the truncations that contained both or the second coiled coil alone were able to interact with hZw10 (see Supplementary Figure S8C).

hZwint-1 interacts with numerous structural kinetochore proteins

Previous studies have found that hZwint-1 can be found in complex with members of the conserved Mis12 and Ndc80 complexes [12,19–21,40]. We have found that hZwint-1 interacts with hMis12, hNnf1 and hDsn1 (three members of the Mis12 complex) as well as hHec1, hSpc24 and hSpc25 (three members of the Ndc80 complex) in our Y2H assay. Whereas the hHec1 interaction has been shown to be direct [42], all other interactions need to be confirmed by an *in vitro* binding assay. The reason that we cannot confidently claim that hZwint-1 interacts directly with all of these proteins is that yeast have homologues of all of the proteins analysed, except for hZwint-1 and hZw10. As such, the interaction may not be direct with each, but rather with a single member of each complex which could potentially bring the DNA-binding and activation domains close enough to produce a positive result. Also, because hZwint-1 is a relatively small protein, it is unlikely that it is able to make direct interactions with all of the proteins identified here. A recent study using recombinant protein demonstrated that hZwint-1 is not able to interact directly with the Mis12 or Ndc80 complexes, but that Blinkin bridges the complexes [12].

hZwint-1 is a stable kinetochore component

Examination of FRAP of other kinetochore proteins has revealed that there are two main types of proteins at the kinetochore: those that are stable and those that are highly dynamic. Mitotic checkpoint proteins such as GFP-hZw10 [39], GFP-Mps1, GFP-Bub3 and GFP-Cdc20 [32] have very rapid recovery at metaphase kinetochores. Kinetochore proteins that do not recover after photobleaching include the centromere proteins CENP-A, CENP-C, CENP-H, CENP-I [23] and CENP-T [45] as well as GFP-Mis12 (see Supplementary Figure S7C) and the Ndc80 complex members, Nuf2-GFP [44], GFP-hHec1 (see Supplementary Figure S7A) and GFP-hSpc24 (see Supplementary Figure S7B). On the basis of the lack of fluorescence recovery, we conclude that hZwint-1 is a stable component of the kinetochore and a structural protein involved in the assembly of the outer kinetochore rather than a mitotic checkpoint protein. This is also supported by the lack of relative hZwint-1 intensity changes at the kinetochore during mitosis (Figure 4C). hZwint-1 kinetochore fluorescence intensity becomes strong through prophase and prometaphase, peaks at metaphase and remains high through anaphase and then decreases at anaphase B and is absent at telophase (Figure 4C). This is in contrast with the dynamic checkpoint proteins Mps1, Bub3 and Cdc20 which all peak at prometaphase unattached kinetochores and decrease upon MT attachment [32].

Model and conclusions

On the basis of published reports and the domains mapped here, we propose the following model for hZwint-1 localization at the kinetochore (Figure 5). Blinkin, Hec1 and Mis12 have been shown to be required for hZwint-1 localization to the kinetochore [11,21,42] and we found that amino acids 40–109 of hZwint-1 are required for kinetochore localization. We have also found that hZwint-1 interacts with members of both the Mis12 and Ndc80 complexes, although it may not be direct, and thus the N-terminus of hZwint-1 may interact with both or one of the complexes through the kinetochore localization domain. hZw10 is located exterior to hZwint-1 at the kinetochore and the region of hZwint-1 involved in this interaction is in the C-terminus of the protein (amino acids 196–236). Thus the N-terminus of hZwint-1 is towards the inner kinetochore, and the C-terminus is towards

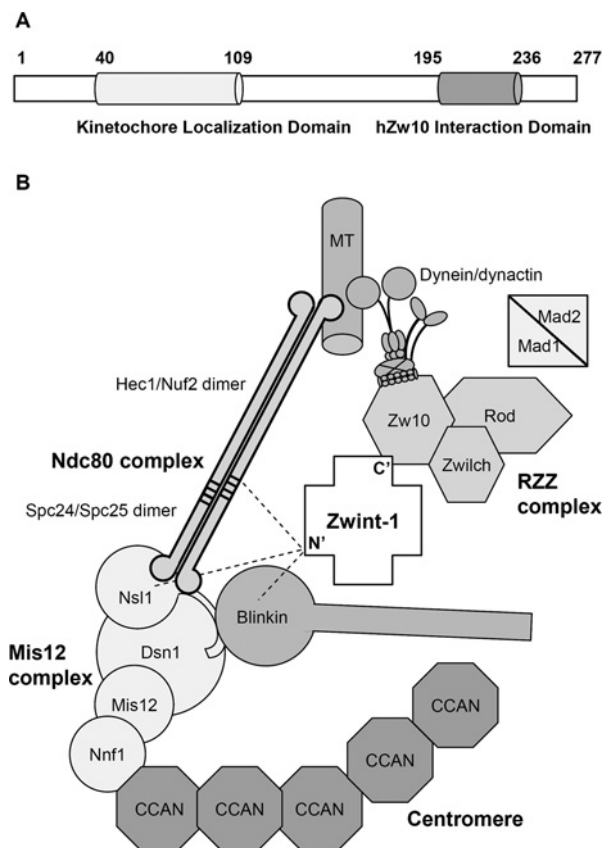


Figure 5 Model of the location of hZwint-1 at the kinetochore

(A) Linear diagram of hZwint-1's functional domains mapped by the mutagenesis screen. hZwint-1 localizes to the kinetochore through the N-terminus (amino acids 40–109) and interacts with hZw10 through the C-terminal coiled-coil domain (amino acids 195–236). (B) hZwint-1 bridges the inner and outer kinetochores similar to that proposed for the Ndc80 complex. hZwint-1 localizes to the kinetochore via its N-terminus which is shown towards the inner kinetochore. hZwint-1 interacts with components of the Ndc80 complex and the Mis12 complex, as well as Blinkin. At this time, it is unknown which of these protein interactions occur through this domain, but possibilities are indicated by the broken line. hZw10, an outer kinetochore protein, interacts with the C-terminus of hZwint-1, so the C-terminus of hZwint-1 should be towards the outer kinetochore. The RZZ complex in turn is required for recruitment of dynein–dynactin and Mad1–Mad2 complexes to the kinetochore. Both dynein–dynactin and the Ndc80 complex are able to bind MTs.

the outer kinetochore. Determination of the protein that binds directly to hZwint-1 through the kinetochore localization domain identified in the present study will clarify the model further.

Mapping the domains of hZwint-1 has provided insight into the structure of the protein and will allow further analysis of the importance of hZwint-1's interactions. Additional insight into the structure of hZwint-1, and the domains mapped in the present study, could be gained by determination of the crystal structure of hZwint-1 protein. Determination of the structure of hZwint-1 will determine whether the outlying mutants in this study are truly involved in hZw10 interaction or kinetochore localization because of complex secondary structure or whether they are negative in the assays employed as a result of improper folding.

AUTHOR CONTRIBUTION

Larissa Vos participated in experimental design, generated the majority of the data, performed data analysis and wrote the paper. Jakub Famulski was responsible for the FRAP

experiment and participated in data analysis and editing of the paper before submission. Gordon Chan supervised and designed the experiments, participated in data analysis and editing of the paper before submission.

ACKNOWLEDGEMENTS

We thank the members of the Chan laboratory for their encouragement and helpful discussion. We acknowledge the gift of ACAs from Dr Marvin Fritzler and Y2H plasmids from Dr Erica Golemis. All microscopy experiments were performed at the Cross Cancer Institute Cell Imaging Facility.

FUNDING

L.J.V. was funded by a PGS-A graduate studentship from the Natural Sciences and Engineering Research Council of Canada [grant number PGS A-265088-2003] and a graduate studentship from the Alberta Cancer Research Institute [grant number 24161]. J.K.F. was funded by a Canadian Graduate Scholarship Award from the Canadian Institute of Health Research [grant number 71295] and a graduate studentship from the Alberta Cancer Research Institute [grant number 23310]. This research was funded by the Canadian Institute of Health Research [grant numbers MOP-57723 and MOP143586], the Alberta Cancer Research Institute [grant number 21594], the Canadian Foundation for Innovation [grant number 9569], the Alberta Heritage Foundation for Medical Research [grant number 200301326], the Natural Sciences and Engineering Research Council of Canada [grant number 355777-08] and the Alberta Science and Research Authority [grant number URSI-05-028-SRI].

REFERENCES

- Nicklas, R. B. (1997) How cells get the right chromosomes. *Science* **275**, 632–637
- Rieder, C. L., Schultz, A., Cole, R. and Sluder, G. (1994) Anaphase onset in vertebrate somatic cells is controlled by a checkpoint that monitors sister kinetochore attachment to the spindle. *J. Cell Biol.* **127**, 1301–1310
- King, R. W., Peters, J. M., Tugendreich, S., Rolfe, M., Hieter, P. and Kirschner, M. W. (1995) A 20S complex containing CDC27 and CDC16 catalyzes the mitosis-specific conjugation of ubiquitin to cyclin B. *Cell* **81**, 279–288
- Sudakin, V., Ganoh, D., Dahan, A., Heller, H., Hershko, J., Luca, F. C., Ruderman, J. V. and Hershko, A. (1995) The cyclosome, a large complex containing cyclin-selective ubiquitin ligase activity, targets cyclins for destruction at the end of mitosis. *Mol. Biol. Cell* **6**, 185–197
- Bharadwaj, R. and Yu, H. (2004) The spindle checkpoint, aneuploidy, and cancer. *Oncogene* **23**, 2016–2027
- Earnshaw, W. C. and Rothfield, N. (1985) Identification of a family of human centromere proteins using autoimmune sera from patients with scleroderma. *Chromosoma* **91**, 313–321
- Foltz, D. R., Jansen, L. E., Black, B. E., Bailey, A. O., Yates, 3rd, J. R. and Cleveland, D. W. (2006) The human CENP-A centromeric nucleosome-associated complex. *Nat. Cell Biol.* **8**, 458–469
- Hori, T., Amano, M., Suzuki, A., Backer, C. B., Welburn, J. P., Dong, Y., McEwen, B. F., Shang, W. H., Suzuki, E., Okawa, K. et al. (2008) CCAN makes multiple contacts with centromeric DNA to provide distinct pathways to the outer kinetochore. *Cell* **135**, 1039–1052
- Okada, M., Cheeseman, I. M., Hori, T., Okawa, K., McLeod, I. X., Yates, 3rd, J. R., Desai, A. and Fukagawa, T. (2006) The CENP-H-I complex is required for the efficient incorporation of newly synthesized CENP-A into centromeres. *Nat. Cell Biol.* **8**, 446–457
- Cheeseman, I. M., Chappie, J. S., Wilson-Kubalek, E. M. and Desai, A. (2006) The conserved KMN network constitutes the core microtubule-binding site of the kinetochore. *Cell* **127**, 983–997
- Kiyomitsu, T., Obuse, C. and Yanagida, M. (2007) Human Blinkin/AF15q14 is required for chromosome alignment and the mitotic checkpoint through direct interaction with Bub1 and BubR1. *Dev. Cell* **13**, 663–676
- Petrovic, A., Pasqualato, S., Dube, P., Krenn, V., Santaguida, S., Cittaro, D., Monzani, S., Massimiliano, L., Keller, J., Tarricone, A. et al. (2010) The MIS12 complex is a protein interaction hub for outer kinetochore assembly. *J. Cell Biol.* **190**, 835–852
- Cheeseman, I. M., Hori, T., Fukagawa, T. and Desai, A. (2008) KNL1 and the CENP-H/I/K complex coordinately direct kinetochore assembly in vertebrates. *Mol. Biol. Cell* **19**, 587–594
- DeLuca, J. G., Gall, W. E., Ciferri, C., Cimini, D., Musacchio, A. and Salmon, E. D. (2006) Kinetochore microtubule dynamics and attachment stability are regulated by Hec1. *Cell* **127**, 969–982
- DeLuca, J. G., Howell, B. J., Canman, J. C., Hickey, J. M., Fang, G. and Salmon, E. D. (2003) Nuf2 and Hec1 are required for retention of the checkpoint proteins Mad1 and Mad2 to kinetochores. *Curr. Biol.* **13**, 2103–2109
- DeLuca, J. G., Moree, B., Hickey, J. M., Kilmartin, J. V. and Salmon, E. D. (2002) hNuf2 inhibition blocks stable kinetochore–microtubule attachment and induces mitotic cell death in HeLa cells. *J. Cell Biol.* **159**, 549–555
- Janke, C., Ortiz, J., Lechner, J., Shevchenko, A., Magiera, M. M., Schramm, C. and Schiebel, E. (2001) The budding yeast proteins Spc24p and Spc25p interact with Ndc80p and Nuf2p at the kinetochore and are important for kinetochore clustering and checkpoint control. *EMBO J.* **20**, 777–791
- McClelland, M. L., Gardner, R. D., Kallio, M. J., Daum, J. R., Gorbisky, G. J., Burke, D. J. and Stukenberg, P. T. (2003) The highly conserved Ndc80 complex is required for kinetochore assembly, chromosome congression, and spindle checkpoint activity. *Genes Dev.* **17**, 101–114
- Cheeseman, I. M., Niessen, S., Anderson, S., Hyndman, F., Yates, 3rd, J. R., Oegema, K. and Desai, A. (2004) A conserved protein network controls assembly of the outer kinetochore and its ability to sustain tension. *Genes Dev.* **18**, 2255–2268
- Kline, S. L., Cheeseman, I. M., Hori, T., Fukagawa, T. and Desai, A. (2006) The human Mis12 complex is required for kinetochore assembly and proper chromosome segregation. *J. Cell Biol.* **173**, 9–17
- Obuse, C., Iwasaki, O., Kiyomitsu, T., Goshima, G., Toyoda, Y. and Yanagida, M. (2004) A conserved Mis12 centromere complex is linked to heterochromatic HP1 and outer kinetochore protein Zwint-1. *Nat. Cell Biol.* **6**, 1135–1141
- Joglekar, A. P., Bouck, D. C., Molk, J. N., Bloom, K. S. and Salmon, E. D. (2006) Molecular architecture of a kinetochore–microtubule attachment site. *Nat. Cell Biol.* **8**, 581–585
- Hemmerich, P., Weidtkamp-Peters, S., Hoischen, C., Schmiedebeg, L., Erliandri, I. and Diekmann, S. (2008) Dynamics of inner kinetochore assembly and maintenance in living cells. *J. Cell Biol.* **180**, 1101–1114
- Cahill, D. P., Lengauer, C., Yu, J., Riggins, G. J., Willson, J. K., Markowitz, S. D., Kinzler, K. W. and Vogelstein, B. (1998) Mutations of mitotic checkpoint genes in human cancers. *Nature* **392**, 300–303
- Chan, G. K., Schaar, B. T. and Yen, T. J. (1998) Characterization of the kinetochore binding domain of CENP-E reveals interactions with the kinetochore proteins CENP-F and hBUBR1. *J. Cell Biol.* **143**, 49–63
- Chen, R. H., Shevchenko, A., Mann, M. and Murray, A. W. (1998) Spindle checkpoint protein Xmad1 recruits Xmad2 to unattached kinetochores. *J. Cell Biol.* **143**, 283–295
- Jablonski, S. A., Chan, G. K., Cooke, C. A., Earnshaw, W. C. and Yen, T. J. (1998) The hBUB1 and hBUBR1 kinases sequentially assemble onto kinetochores during prophase with hBUBR1 concentrating at the kinetochore plates in mitosis. *Chromosoma* **107**, 386–396
- Li, Y. and Benzra, R. (1996) Identification of a human mitotic checkpoint gene: hMAD2. *Science* **274**, 246–248
- Taylor, S. S., Ha, E. and McKeon, F. (1998) The human homologue of Bub3 is required for kinetochore localization of Bub1 and a Mad3/Bub1-related protein kinase. *J. Cell Biol.* **142**, 1–11
- Taylor, S. S. and McKeon, F. (1997) Kinetochore localization of murine Bub1 is required for normal mitotic timing and checkpoint response to spindle damage. *Cell* **89**, 727–735
- Sudakin, V., Chan, G. K. and Yen, T. J. (2001) Checkpoint inhibition of the APC/C in HeLa cells is mediated by a complex of BUBR1, BUB3, CDC20, and MAD2. *J. Cell Biol.* **154**, 925–936
- Howell, B. J., Moree, B., Farrar, E. M., Stewart, S., Fang, G. and Salmon, E. D. (2004) Spindle checkpoint protein dynamics at kinetochores in living cells. *Curr. Biol.* **14**, 953–964
- Starr, D. A., Saffery, R., Li, Z., Simpson, A. E., Choo, K. H., Yen, T. J. and Goldberg, M. L. (2000) hZwint-1, a novel human kinetochore component that interacts with hZW10. *J. Cell Sci.* **113**, 1939–1950
- Chan, G. K., Jablonski, S. A., Starr, D. A., Goldberg, M. L. and Yen, T. J. (2000) Human Zw10 and ROD are mitotic checkpoint proteins that bind to kinetochores. *Nat. Cell Biol.* **2**, 944–947
- Williams, B. C., Li, Z., Liu, S., Williams, E. V., Leung, G., Yen, T. J. and Goldberg, M. L. (2003) Zwilch, a new component of the ZW10/ROD complex required for kinetochore functions. *Mol. Biol. Cell* **14**, 1379–1391
- Karess, R. (2005) Rod–Zw10–Zwilch: a key player in the spindle checkpoint. *Trends Cell Biol.* **15**, 386–392
- Buffin, E., Lefebvre, C., Huang, J., Gagou, M. E. and Karess, R. E. (2005) Recruitment of Mad2 to the kinetochore requires the Rod/Zw10 complex. *Curr. Biol.* **15**, 856–861
- Starr, D. A., Williams, B. C., Hays, T. S. and Goldberg, M. L. (1998) ZW10 helps recruit dyactin and dynein to the kinetochore. *J. Cell Biol.* **142**, 763–774
- Famulski, J. K., Vos, L., Sun, X. and Chan, G. (2008) Stable hZW10 kinetochore residency, mediated by hZwint-1 interaction, is essential for the mitotic checkpoint. *J. Cell Biol.* **180**, 507–520

- 40 Kops, G. J., Kim, Y., Weaver, B. A., Mao, Y., McLeod, I., Yates, 3rd, J. R., Tagaya, M. and Cleveland, D. W. (2005) ZW10 links mitotic checkpoint signaling to the structural kinetochore. *J. Cell Biol.* **169**, 49–60
- 41 Wang, H., Hu, X., Ding, X., Dou, Z., Yang, Z., Shaw, A. W., Teng, M., Cleveland, D. W., Goldberg, M. L., Niu, L. and Yao, X. (2004) Human Zwint-1 specifies localization of Zeste White 10 to kinetochores and is essential for mitotic checkpoint signaling. *J. Biol. Chem.* **279**, 54590–54598
- 42 Lin, Y. T., Chen, Y., Wu, G. and Lee, W. H. (2006) Hec1 sequentially recruits Zwint-1 and ZW10 to kinetochores for faithful chromosome segregation and spindle checkpoint control. *Oncogene* **25**, 6901–6914
- 43 Liu, S. T., Chan, G. K., Hittle, J. C., Fujii, G., Lees, E. and Yen, T. J. (2003) Human MPS1 kinase is required for mitotic arrest induced by the loss of CENP-E from kinetochores. *Mol. Biol. Cell* **14**, 1638–1651
- 44 Hori, T., Haraguchi, T., Hiraoka, Y., Kimura, H. and Fukagawa, T. (2003) Dynamic behavior of Nuf2–Hec1 complex that localizes to the centrosome and centromere and is essential for mitotic progression in vertebrate cells. *J. Cell Sci.* **116**, 3347–3362
- 45 Hellwig, D., Munch, S., Orthaus, S., Hoischen, C., Hemmerich, P. and Diekmann, S. (2008) Live-cell imaging reveals sustained centromere binding of CENP-T via CENP-A and CENP-B. *J. Biophotonics* **1**, 245–254

Received 20 January 2011/16 February 2011; accepted 23 February 2011

Published as BJ Immediate Publication 23 February 2011, doi:10.1042/BJ20110137

SUPPLEMENTARY ONLINE DATA

hZwint-1 bridges the inner and outer kinetochore: identification of the kinetochore localization domain and the hZw10-interaction domain

Larissa J. VOS*, Jakub K. FAMULSKI*¹ and Gordon K. T. CHAN*^{†‡2}

*Department of Oncology, Faculty of Medicine and Dentistry, University of Alberta, 11560 University Avenue, Edmonton, Alberta, Canada, T6G 1Z2, †School of Cancer, Engineering and Imaging Sciences, University of Alberta, Edmonton, Alberta, Canada, T6G 2B7, and ‡Experimental Oncology, Cross Cancer Institute, 11560 University Avenue, Edmonton, Alberta, Canada T6G 1Z2

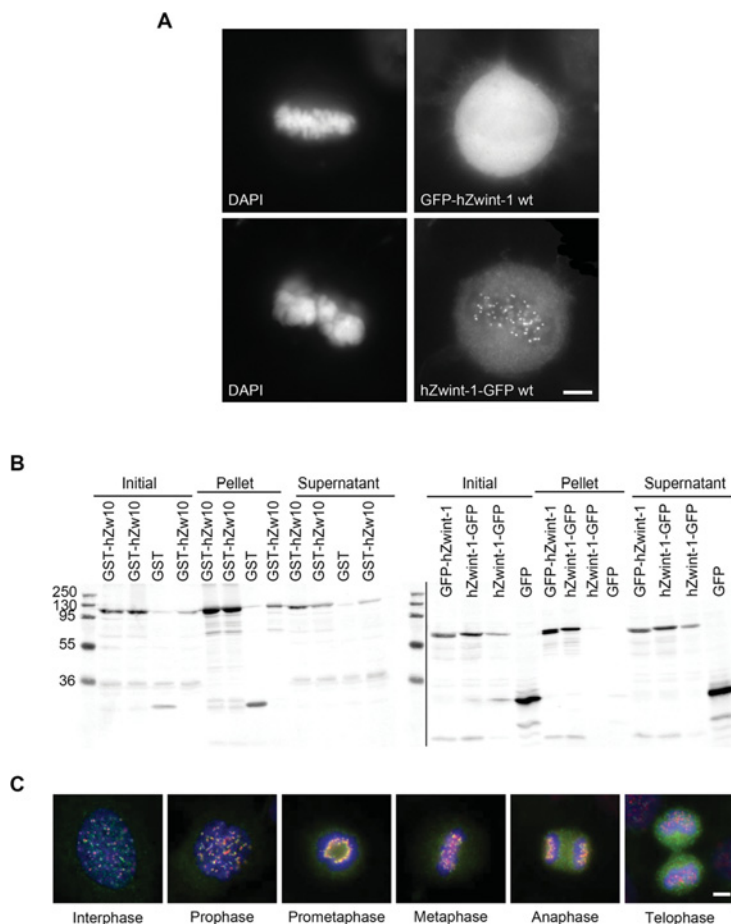


Figure S1 Fusion of GFP to the N-terminus of hZwint-1 interferes with its ability to localize to the kinetochore

(A) HeLa cell coverslips were transfected with either GFP-hZwint-1 or hZwint-1-GFP fusion constructs for 24 h, then were fixed, permeabilized and stained with DAPI to visualize the DNA. Cells were analysed by fluorescence microscopy to determine whether the GFP-fusion protein was able to localize to the kinetochore. GFP-hZwint-1 showed no subcellular localization, but rather was diffuse throughout the cell. hZwint-1-GFP, in contrast, exhibited the expected double-dot staining typical of kinetochore proteins. Scale bar, 5 μ m. (B) Control Western immunoblot showing that the location of the GFP tag did not affect hZwint-1 pull-down by GST-hZw10 and that GST alone was not able to pull down hZwint-1-GFP and neither was GFP alone pulled down by GST-hZw10. Initial samples are 5% of lysate before addition of glutathione-Sepharose beads, pellet is total bound proteins and supernatant is 5% of lysate after beads were pelleted. The two blot images are from different channels of the same blot. The molecular-mass protein ladder (masses indicated in kDa) only shows up in the 700 channel and has been placed beside the GFP 800 channel blot for reference. (C) Expansion of Figure 1(A) of the main text. Each cell phase is merged with hZwint-1 in green, ACA in red and DAPI in blue. Yellow indicates overlap of hZwint-1 and ACA signal. hZwint-1 localizes to the kinetochore from prophase until anaphase and, although there is some overlap of signal, hZwint-1 is exterior to ACA as clearly seen in prophase and metaphase. Scale bar, 5 μ m.

¹ Present address: Department of Biological Sciences, University of Alberta, Edmonton, Alberta, Canada, T6G 2E9

² To whom correspondence should be addressed (email Gordon.Chan@albertahealthservices.ca).

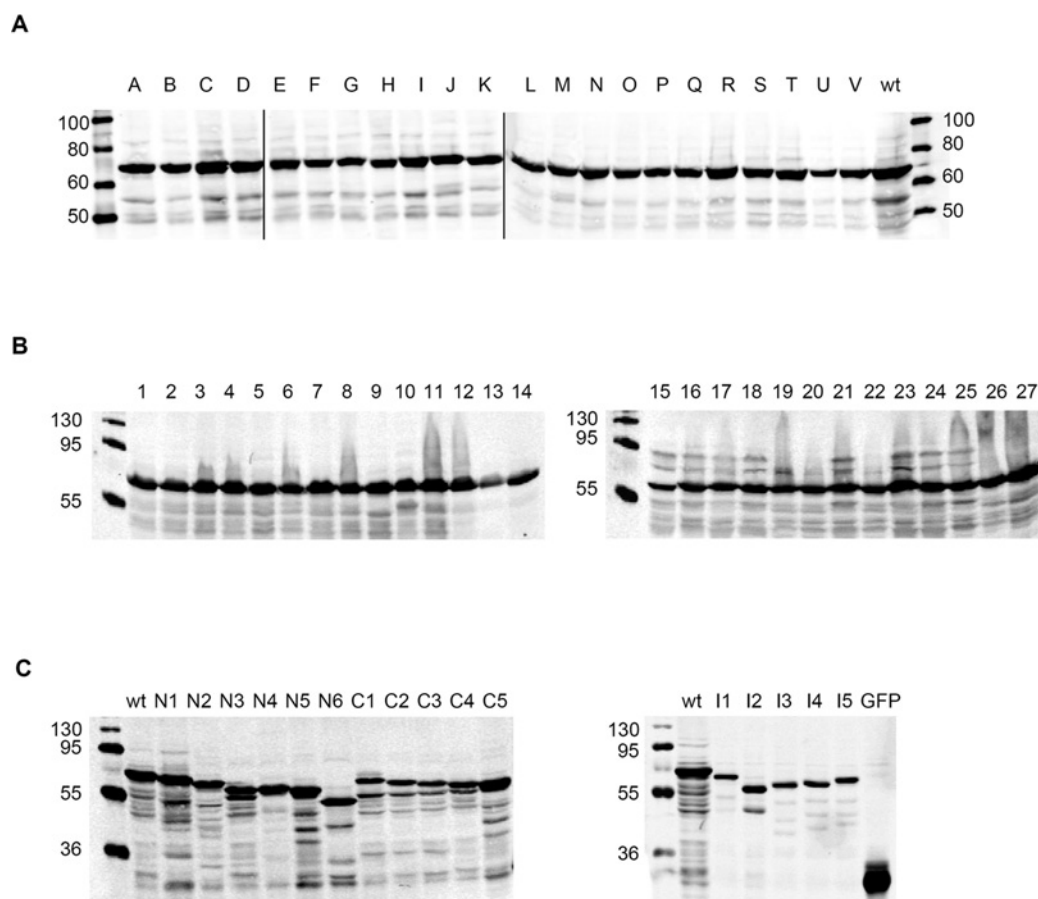


Figure S2 hZwint-1 mutant library Western blot analysis

Immunoblots of transfected HEK-293 lysate showing expression of hZwint-1-GFP fusion proteins. All mutant constructs of hZwint-1 show expression at the expected size. GFP-fusion proteins were detected with IR800-conjugated anti-GFP antibody. Molecular-mass markers, detected in the same channel, are shown on each blot (masses indicated in kDa). wt, wild-type.

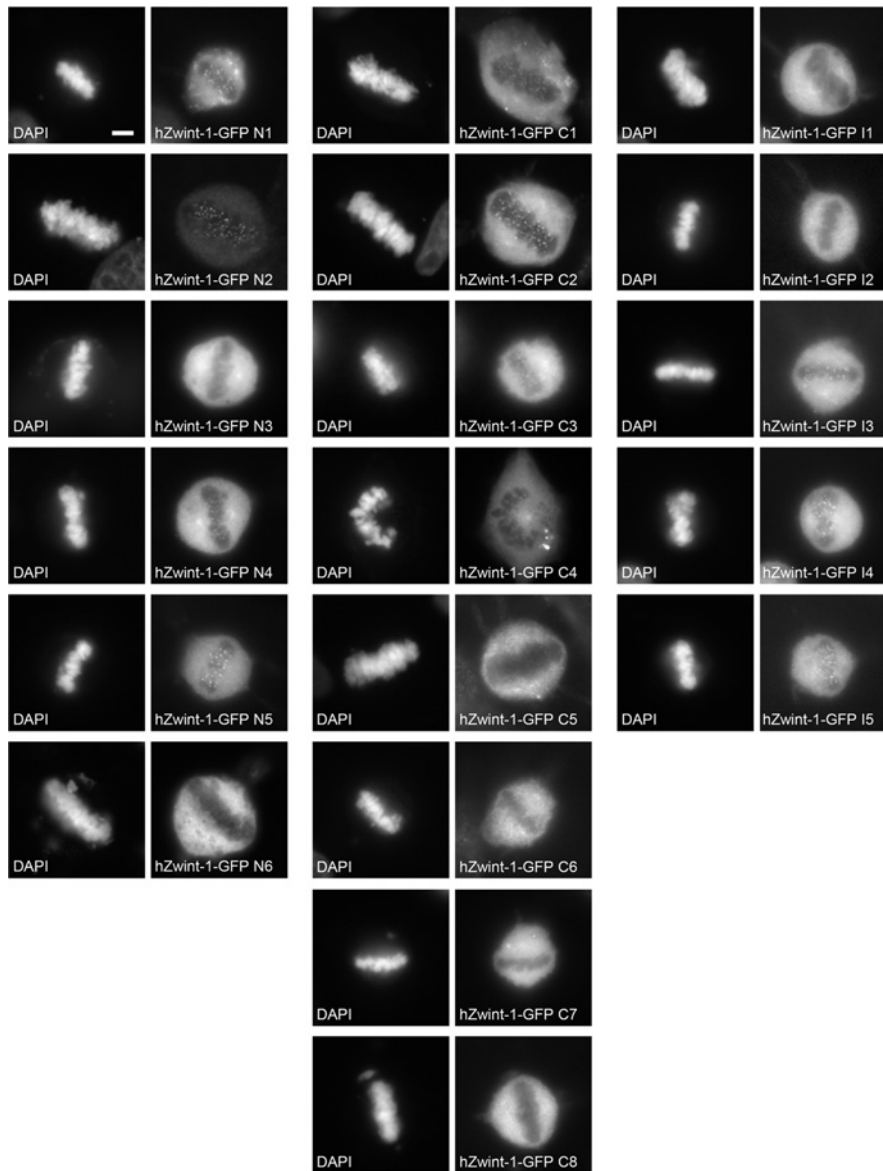


Figure S3 Truncation and internal deletion hZwint-1 mutant library fluorescence analysis

HeLa cells were transfected with hZwint-1-GFP mutants, harvested, stained with DAPI to visualize the DNA and analysed by fluorescence microscopy for the ability to localize to the kinetochore. Positive localization is seen as double-dot staining. Scale bar, 5 μm .

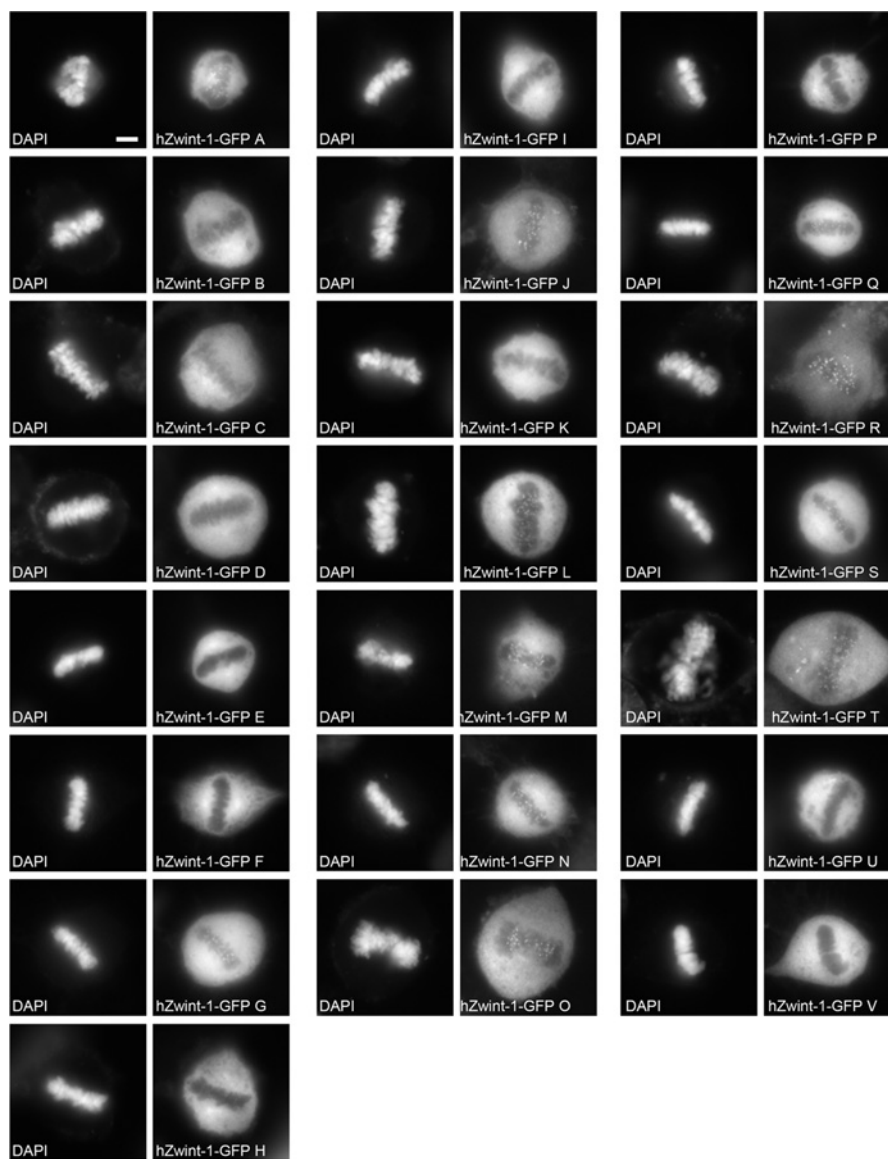


Figure S4 Random insertion hZwint-1 mutant library fluorescence analysis

HeLa cells were transfected with hZwint-1-GFP mutants, harvested, stained with DAPI to visualize the DNA and analysed by fluorescence microscopy for the ability to localize to the kinetochore. Positive localization is seen as double-dot staining. Scale bar, 5 μ m.

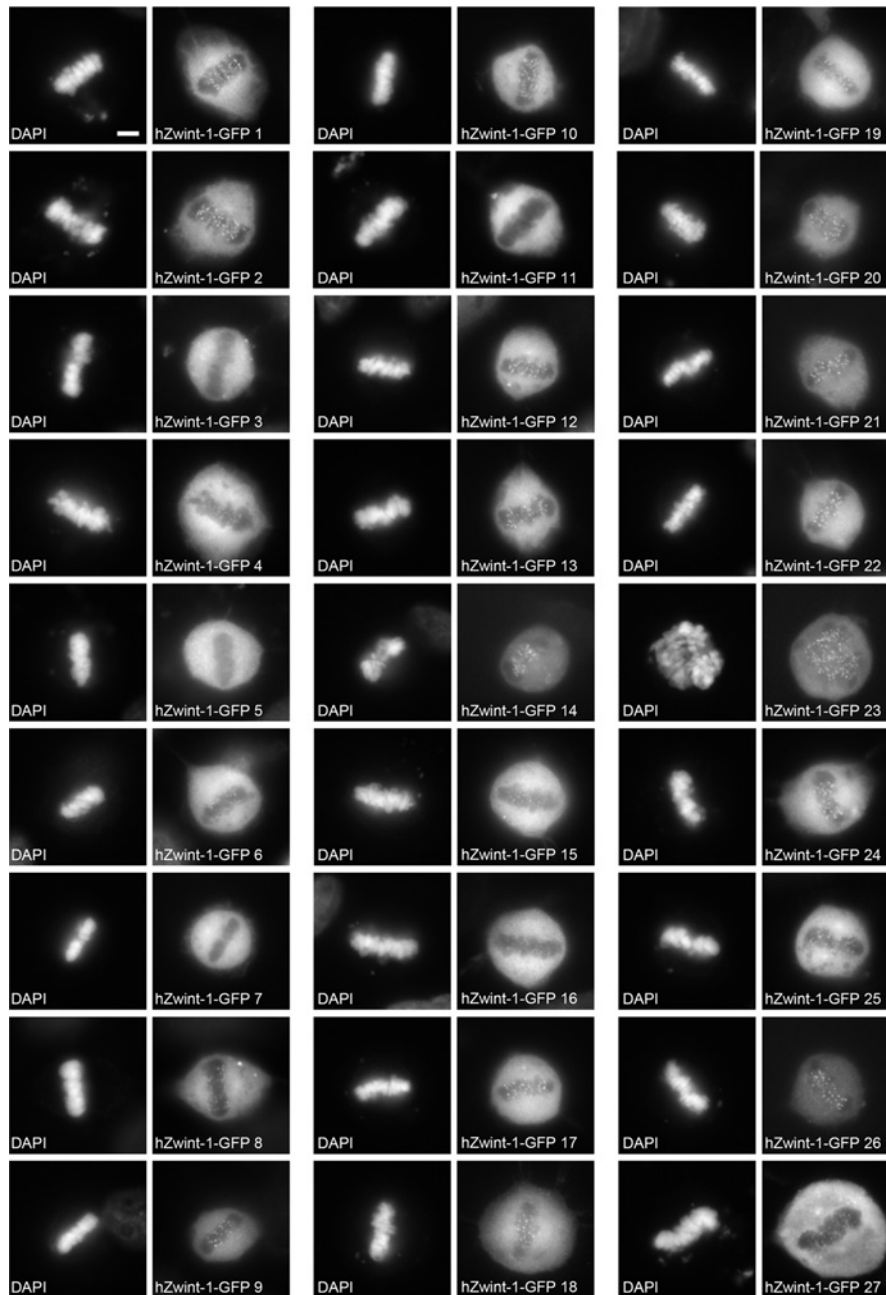


Figure S5 Site-directed hZwint-1 mutant library fluorescence analysis

HeLa cells were transfected with hZwint-1-GFP mutants, harvested, stained with DAPI to visualize the DNA and analysed by fluorescence microscopy for the ability to localize to the kinetochore. Positive localization is seen as double-dot staining. Scale bar, 5 μm .

COLOUR

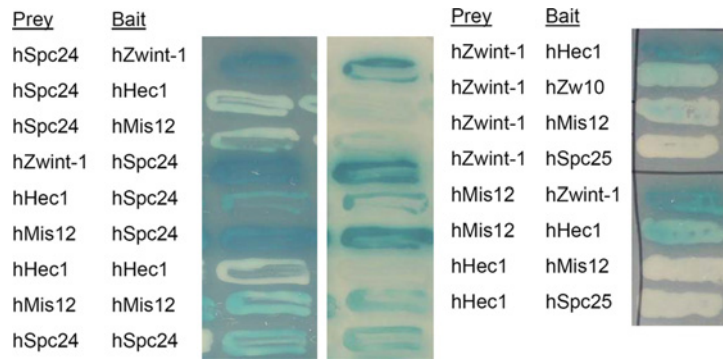


Figure S6 hZwint-1 interacts with several kinetochore components

Representative LexA Y2H experiments between wild-type kinetochore proteins. Interactions were scored by blue/white colour on X-Gal drop-out plates. hZwint-1 was found to interact strongly with hSpc24, hHec1 and hMis12 and moderately with hZw10. The possibility of false positives was checked by transformation of bait construct with empty prey vector and prey construct with empty bait vector. A summary of all interactions found by Y2H analysis are in Table 5 of the main text.

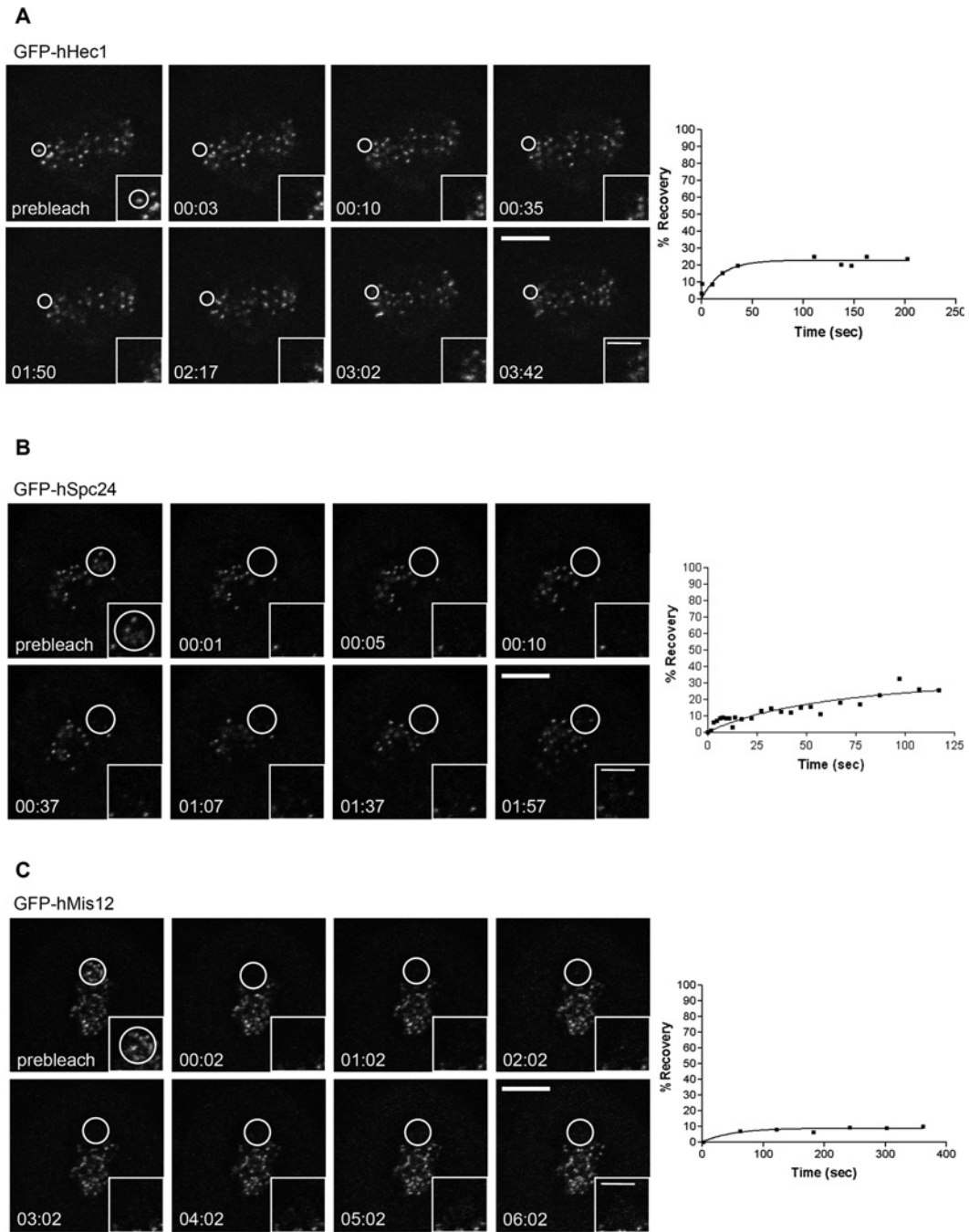


Figure 7 hHec1, hSpc24 and hMis12 are stable kinetochore components

(A) Stills from a live-cell photobleaching movie of GFP-hHec1 and plot of fluorescence recovery following laser photobleaching. GFP-hHec1 does not recover after photobleaching (maximum ~20%), indicating that it is a stable kinetochore component. (B) Stills from a live-cell photobleaching movie of GFP-hSpc24 and plot of fluorescence recovery following laser photobleaching. GFP-hSpc24 does not recover after photobleaching (maximum ~25%), indicating that it is a stable kinetochore component. Area bleached is indicated by a circle on each image. The time of image acquisition is indicated on each panel (min:s) with laser photobleaching occurring at time 00:00. Large scale bar, 10 μm ; inset scale bar, 5 μm . (C) Stills from a live-cell photobleaching movie of GFP-hMis12 and plot of fluorescence recovery following laser photobleaching. GFP-hMis12 does not recover after photobleaching (maximum ~10%), indicating that it is a stable kinetochore component. In all panels, the area bleached is indicated by a circle on each still image. The time of image acquisition is indicated on each still (min:s) with laser photobleaching occurring at time 00:00. Large scale bar, 10 μm ; inset scale bar, 5 μm .

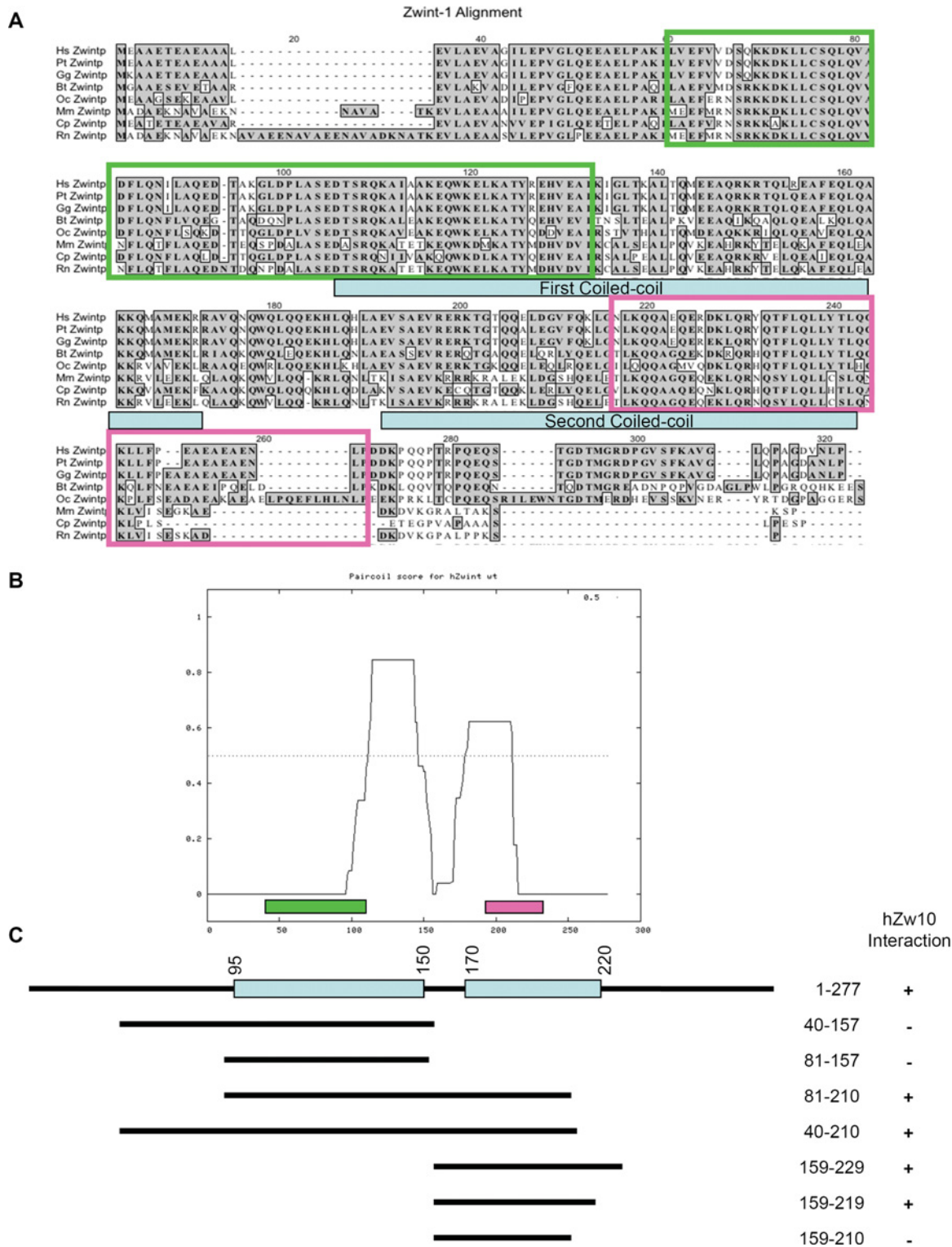


Figure S8 hZwint-1 protein is predicted to contain two coiled-coil domains

(A) ClustalW alignment of hZwint-1 protein showing homology and similarity in sequence generated with MacVector. Outlined in green is the kinetochore localization domain (amino acids 40–109) and in pink is the hZw10-interaction domain (amino acids 195–236). The coiled-coil domains are shown with blue boxes over the aligned sequence. Hs Zwintp, *Homo sapiens* (human) (NP_008988.2); Pt Zwintp, *Pan troglodytes* (chimpanzee) (XP_507799.2); Gg Zwintp, *Gorilla gorilla* (gorilla) (ENSGGOG00000007258); Bt Zwintp, *Bos taurus* (ox/cow) (DAA14988.1); Oc Zwintp, *Oryctolagus cuniculus* (European rabbit) (ENSOCUG00000006806); Mm Zwintp, *Mus musculus* (mouse) (AAH34870.1); Cp Zwintp, *Cavia porcellus* (guinea pig) (ENSCPOG00000009580); Rn Zwintp, *Rattus norvegicus* (rat) (NP_671479.1). (B) Paircoil of hZwint-1 protein showing the location of predicted coiled-coil domains [1]. Highlighted in green is the kinetochore localization domain (amino acids 40–109) and in pink is the hZw10-interaction domain (amino acids 195–236). (C) Schematic diagram of the full-length hZwint-1 protein with coiled-coil domains indicated and truncation mutants covering each coiled-coil individually and in series. Amino acids and ability to interact with hZw10 by the Y2H assay are indicated.

REFERENCE

- 1 Lupas, A. (1997) Predicting coiled-coil regions in proteins. *Curr. Opin. Struct. Biol.* **7**, 388–393

Received 20 January 2011/16 February 2011; accepted 23 February 2011
Published as BJ Immediate Publication 23 February 2011, doi:10.1042/BJ20110137